Article

Not peer-reviewed version

Genome-Wide Characterization and Transcriptional Analyses of the Calmodulin and Calmodulin-Like Protein Family in Canavalia rosea Provide Insight into Their Potential Roles in Abiotic Stress Tolerance

Qianqian Ding , Zengwang Huang * , Zhengfeng Wang , Shuguang Jian , Mei Zhang *

Posted Date: 4 October 2024

doi: 10.20944/preprints202410.0293.v1

Keywords: Calmodulin; Calmodulin-like protein; Ecological adaptability; Yeast heterogeneous expression; Canavalia rosea

Article

Genome-wide characterization and transcriptional analyses of the calmodulin and calmodulin-like protein family in *Canavalia rosea* provide insight into their potential roles in abiotic stress tolerance

Qianqian Ding [1,2,†], Zengwang Huang [1,2,†], Zhengfeng Wang [1,3,4], Shuguang Jian [1,3] and Mei Zhang [1,3,*]

[1] Guangdong Provincial Key Laboratory of Applied Botany&South China Agricultural Plant Molecular Analysis and Genetic Improvement, South China Botanical Garden, Chinese Academy of Sciences, Guangzhou 510650, China;
[2] University of the Chinese Academy of Sciences, Beijing 100039, China;
[3] CAS Engineering Laboratory for Vegetation Ecosystem Restoration on Islands and Coastal Zones, South China Botanical Garden, Chinese Academy of Sciences, Guangzhou 510650, China;
[4] Southern Marine Science and Engineering Guangdong Laboratory (Guangzhou), Guangzhou 511458, China;
* Correspondence: and requests for materials should be addressed to Mei Zhang (zhangmei@scbg.ac.cn).
[#] These two authors contributed equally.

Abstract: Calmodulins (CaMs) and calmodulin-like-proteins (CMLs) belong to families of calcium-sensors that act as calcium-ion (Ca^{2+}) signal-decoding proteins and regulate downstream target proteins. As a tropical halophyte, *Canavalia rosea* shows great resistance to multiple abiotic stresses, including high salinity-alkaline, extreme drought, heat, and intense sunlight. However, investigations of calcium ion signal transduction involved in the stress responses of *C. rosea* are limited. The *CaM* and *CML* gene families have been identified and characterized in many species. Nevertheless, there is limited available information about these genes in *C. rosea*. In this study, a bioinformatic analyses, including the gene structures, conserved domains, phylogenetic relationships, chromosome distribution, and gene synteny, was comprehensively performed to identify and characterize the *CrCaM* and *CrCML* gene members. A spatio-temporal expression analysis in different organs and environmental conditions were then assayed using the RNA sequencing technique. Additionally, several *CrCaM* and *CrCML* members were then cloned and functionally characterized using the yeast heterogeneous expression system, and some of them were found to change the tolerance of yeast to heat, salt, alkaline, and high osmotic stresses. Furthermore, this indicated that the *CrCaMs* and *CrCMLs* play important roles in stress resistance. The results of this study provide a foundation for understanding the possible roles of plant *CaM* and *CML* genes, especially for halophyte *C. rosea* natural ecological adaptability. This study also provides a theoretical basis for further study of the physiological functions of plant *CrCaM*s and *CrCML*s that are involved in multiple abiotic stresses.

Keywords: calmodulin; calmodulin-like protein; Ecological adaptability; yeast heterogeneous expression; *Canavalia rosea*

1. Introduction

In plants, calcium ions (Ca^{2+}) act as a secondary messenger, playing vital roles in intracellular signaling during various developmental processes and in response to both biotic and abiotic stimuli [1]. The calcium signal is transferred by a series of Ca^{2+}-binding proteins, among them calmodulin (CaM) and calmodulin-like protein (CML) are major calcium sensors that have been shown to be involved in a wide variety of environmental responses and physiological activities [2,3]. The CaM and CML proteins comprise the EF-hand motifs with helix-loop-helix structures for Ca^{2+}-binding, acting as sensors in interpreting encrypted Ca^{2+} signals [4–6]. Studies have shown that CaM is one of the most conserved proteins with 4 EF-hand domains in all eukaryotes [2,7]. In contrast, CML is

doi:10.20944/preprints202410.0293.v1

relatively less conservative, containing 1–6 degenerated EF-hand domains [8,9], and it only exists in plants or some protists [3,4].

Due to their sessile characteristic, plants are inevitably challenged by multiple biotic invasions and environmental changes under normal or stress conditions. These challenges are typically caused by transient fluctuations in the cytosolic Ca^{2+} ($[Ca^{2+}]_{cyt}$) levels, and the changes of Ca^{2+} signatures are decoded by Ca^{2+}-binding proteins, including CaM and CML [10]. There are five types of Ca^{2+}-binding proteins with EF-hand motifs, including calmodulin (CaMs), calmodulin-like proteins (CMLs), calcium-dependent protein kinase (CDPKs), calcium dependent protein kinase related kinase (CRK), and calcineurin B-like proteins (CBLs) [5,9]. CaM is a small well-characterized Ca^{2+} sensor and has multi-functions to respond to different biotic and abiotic stimuli. In addition, it is evolutionarily conserved and possesses good heat and acid stability but lacks its own catalytic activity [10]. CaM can bind to target proteins and control its target proteins by protein–protein interactions or by changing their gene expressions [10,11]. In contrast, CML has greater variability, and its structure is not so conservative. Additionally, convincing evidence has emerged that this type of protein plays central and highly specific roles in coordinating the environmental responses of plants [8,9].

Plant CaM and CML gene families have been identified and characterized in various species, including Arabidopsis [12], rice [13], and other green lineages from algae to land plants [3,14]. *Canavalia rosea* belongs to the family of Leguminosae and is characterized as a pioneer species for tropical coastal saline vegetation construction due to its wide ecological adaptability and potential nitrogen fixation ability [15,16]. However, there are no reports on the Ca^{2+}-binding protein members and their functions in *C. rosea*, especially regarding the ecological adaptation to extreme adversity. Previous studies have summarized the potential roles of plant *CaM*s and *CML*s in responding to various environmental stresses [17–20], with extensive research indicating that these genes may play key roles in salt or drought tolerance [21–26], or even sensitivities [27,28], and other abiotic stresses responding, such as heat [17] and freezing [23]. In recent years, some *CaM* and *CML* gene families have been identified in special habitat plants, including hydrophyte *Saccharina japonicaa* [29] and the sacred lotuses [30], halophytes *Paspalums vaginatum* [31] and *Nitraria sibirica* [32]. The related results provide insights into the potential function of these plant *CaM*/*CML* genes and their possible roles in the molecular mechanisms of extreme tolerance to abiotic stresses. We previously identified a series of *C. rosea*'s gene families, and we primarily focused on this specie's water shortage stress [16,33], heat shock response [34,35], and heavy metal detoxification as a halophyte [36–39]. In this study, to address the possible roles of the *C. rosea* Ca^{2+} signal system for its ecological adaptability to tropical coral extreme habitats, we separated the *CrCaM*/*CrCML* gene family from the entire *C. rosea* genome. The genes' chromosomal locations, synteny, and the phylogenetic relationships were also retrieved based on genome sequencing data. In addition, the expression levels of *CrCaM*/*CrCML* in different tissues were analyzed using an RNA-Seq analysis. This study provides the theoretical molecular mechanisms underlying *C. rosea*'s stress resistance, particularly the pivotal regulatory factors in the Ca^{2+} signal transduction pathway, paving the way for further genetic breeding of salt and alkali tolerance crops.

2. Results

2.1. Genome-Wide Identification and Annotation of the CaMs and CMLs in C. rosea

In total, seven CrCaMs and 44 CrCMLs were identified through Pfam, and SMART search predicted the presence of the EF-hand domain pair (PF13499). Their corresponding genes were finally selected as the order of their chromosomal locations (*CrCaM1* to *CrCaM7* and *CrCML1* to *CrCML44*) (Table 1). The amino acid length of the CrCaMs/CrCMLs proteins ranged from 81 aa (CrCML3) to 288 aa (CrCML6), the molecular weights ranged from 9.21 kDa (CrCML3) to 33.26 kDa (CrCML6), and the theoretical isoelectric points ranged from 3.89 (CrCaM3) to 8.79 (CrCML35) (Table 1). In addition, only CrCML9 (8.70), CrCML35 (8.79), and CrCML43 (7.63) were considered to be basic (pI > 7). The instability index ranged between 59.01 (CrCML26) and 14.27 (CrCML44) and averaged approximately 35, and a small portion of members (19 members, 36%) had a high instability index (II) (> 40). This result indicated that most of these members might be stable. The aliphatic index (AI) assessment showed that most members had lower values, indicating that only a small number of these proteins appeared to be lipophilic or hydrophobic. Accordingly, only one member (CrCML31) had calculated grand average of hydropathy (GRAVY) values of greater than 0 (0.057), implying that most of these proteins were quite hydrophilic. The contents of the disordered amino acids reflected the regularity of protein structure, and we also predicted the 3D structures (Figure S1) and calculated the disordered amino acid contents of all of the CrCaM/CrCML proteins. Obviously, seven CrCaMs presented typical dumbbell structures, and only half of the CrCMLs also showed dumbbell structures, while some of the CrCMLs presented disordered 3D structures, such as CrCML2, CrCML4, CrCML6, CrCML9, CrCML10, CrCML11, CrCML15, CrCML19, CrCML20, CrCML21, CrCML24, CrCML25, CrCML27, CrCML32, CrCML36, CrCML37, CrCML38, and CrCML43 (Figure S1). Compared with some typical intrinsically disordered protein families members identified from *C. rosea* [33,39], the disordered amino acid contents of the CrCaMs/CrCMLs were relatively low (most of them were below 50, Table 1), which indicated that the CrCaM/CrCML proteins had stable 3D structures for their functional guarantee. Moreover, the subcellular localization prediction that the CrCaM/CrCML members were widely distributed within most of the cell organelles further supported their biological functional diversities and universalities.

Table 1. Nomenclature and subcellular localization of CrCaMs and CrCMLs identified from *C. rosea* genome.

Name	**Locus**	**Protein length**	**Major amino acids (aa, %)**	**Mw (kDa)**	**PI**	**II**	**AI**	**GRAVY**	**Disordered aa (%)**	**WoLF_PSORT**	**Plant-PLoc**
CrCaM1	03T007739	149	D(12.8%),E(12.8%),L(7.4%)	16.85	4.11	24.52	69.40	-0.619	32.89	nucl: 4, mito: 4, extr: 3, cyto: 2	Endoplasmic reticulum
CrCaM2	04T011067	171	E(14.0%),D(9.9%),L(8.8%)	19.68	4.05	38.15	84.33	-0.337	30.99	cyto: 6, chlo: 3, nucl: 3, plas: 1	Chloroplast
CrCaM3	04T011068	150	E(15.3%),D(12.0%),L(9.3%)	17.04	3.89	46.07	89.00	-0.331	25.33	cyto: 8, chlo: 2, extr: 1, E.R.: 1, cysk: 1	Nucleus
CrCaM4	04T013039	150	E(14.7%),D(12.7%),L(8.0%)	17.03	4.03	35.84	81.20	-0.487	31.33	chlo: 5, cyto: 4.5, cyto_nucl: 3.33333, extr: 3	Endoplasmic reticulum
CrCaM5	06T017463	190	D(11.1%),D(10.5%),L(10.0%)	21.59	4.14	33.12	80.58	-0.268	42.11	chlo: 6, plas: 2, nucl: 1.5, cysk_nucl: 1.5, cyto: 1, mito: 1, vacu: 1	Chloroplast
CrCaM6	07T020185	149	E(13.4%),D(12.1%),L(7.4%)	16.86	4.12	25.82	69.40	-0.619	32.89	nucl: 4, mito: 4, extr: 3, cyto: 2	Endoplasmic reticulum

CrCaM7	11T029359	149	D(12.8%),E(12.8%),A(7.4%), L(7.4%)	16.83	4.11	23.23	70.07	-0.602	32.89	cyto: 4, mito: 4, nucl: 3, extr: 2	Endoplasmic reticulum
CrCML1	01T000055	177	N(10.7%),D(10.7%),E(8.5%), G(8.5%)	19.60	4.23	39.80	59.49	-0.808	58.19	nucl: 6, chlo: 4, mito: 2, extr: 2	Nucleus
CrCML2	01T000134	187	D(8.2%),S(8.2%),E(9.1%), G(9.1%)	20.52	4.30	45.03	75.56	-0.396	55.61	chlo: 10, mito: 4	Nucleus
CrCML3	01T001229	81	E(12.3%),D(11.1%),L(11.1%)	9.21	4.62	41.03	85.43	-0.593	22.22	cyto: 5, nucl: 3.5, chlo: 3, cysk_nucl: 2.5, extr: 1	Cytoplasm
CrCML4	01T001582	191	S(10.5%),D(9.9%),G(8.4%)	21.71	5.12	49.75	56.65	-0.700	65.97	mito: 9, nucl: 4	Chloroplast
CrCML5	01T001986	160	L(11.2%),D(8.1%),G(8.1%)	17.62	4.21	35.31	83.56	-0.124	38.75	nucl: 5.5, nucl_plas: 4, cyto: 3.5, cyto_E.R.: 2.5, mito: 2, plas: 1.5	Nucleus
CrCML6	01T002018	288	E(11.1%),L(9.7%),F(8.7%)	33.26	4.97	42.59	76.56	-0.316	42.01	cyto: 5, chlo: 3, plas: 3, E.R.: 2	Chloroplast
CrCML7	01T002045	163	L(12.3%),A(11.0%),E(9.2%)	18.13	4.66	39.69	84.54	-0.315	43.56	plas: 5, nucl_plas: 5, nucl: 3, cyto: 2, mito: 2, chlo: 1	Nucleus
CrCML8	01T002566	179	L(11.2%),E(10.6%),N(7.8%)	20.41	4.37	46.73	87.65	-0.046	42.46	chlo: 11, cyto: 1, extr: 1	Chloroplast
CrCML9	01T002767	193	D(9.3%),K(9.3%),S(8.8%)	22.32	8.70	39.56	60.57	-0.627	60.10	nucl: 7.5, cyto_nucl: 4.5, chlo: 4, mito: 2	Cytoplasm
CrCML10	01T003442	155	G(14.2%),D(12.9%),L(7.7%)	16.86	4.81	31.39	66.71	-0.414	72.90	cyto: 6, mito: 4, chlo: 2, nucl: 1	Chloroplast
CrCML11	02T004181	197	D(10.7%),L(9.6%),S(9.6%)	21.89	4.55	41.87	72.79	-0.406	63.45	nucl: 7, cyto: 3, mito: 2, extr: 2	Cytoplasm

CrCML 12	02T004464	187	G(10.7%),L(10.7%),E(10.2%)	20.98	4.69	36.33	78.13	-0.415	45.99	cyto: 11, nucl: 1, mito: 1	Cytoplasm
CrCML 13	02T004981	139	L(14.4%),E(10.8%),D(9.4%)	16.00	4.34	27.74	80.58	-0.491	34.53	nucl: 5, mito: 5, chlo: 3	Cytoplasm
CrCML 14	02T006679	214	L(9.8%),S(9.8%),D(9.3%)	24.15	5.18	32.02	76.50	-0.309	47.20	chlo: 11, nucl: 1, mito: 1	Cytoplasm
CrCML 15	03T007802	152	D(11.8%),G(10.5%),E(9.9%)	17.03	4.32	15.81	73.09	-0.447	32.24	chlo: 4, extr: 4, nucl: 2, cyto: 2, mito: 2	Cytoplasm
CrCML 16	03T007833	223	S(13.9%),D(9.4%),V(9.0%)	24.55	4.63	48.90	73.32	-0.526	60.54	chlo: 5, cyto: 5, nucl: 2, mito: 1	Chloroplast
CrCML 17	03T008082	148	E(14.2%),D(10.1%),I(9.5%)	17.00	4.14	38.60	84.39	-0.443	27.03	cyto: 13	Chloroplast
CrCML 18	03T009031	149	E(16.1%),D(10.7%),L(10.7%)	16.93	4.02	44.45	83.09	-0.448	38.26	cyto_nucl: 5.83333, chlo: 4, nucl: 4, cyto: 3.5, cyto_E.R.: 2.83333	Chloroplast
CrCML 19	03T009705	220	L(10.5%),E(8.6%),I(8.6%)	25.58	5.69	27.67	86.00	-0.378	41.82	cyto: 10, mito: 2, chlo: 1	Chloroplast
CrCML 20	03T010270	182	L(12.1%),D(8.8%),E(8.8%)	20.31	4.37	39.87	88.41	-0.234	41.21	mito: 7.5, chlo_mito: 7, chlo: 5.5	Nucleus
CrCML 21	03T010292	206	L(10.2%),S(10.2%),D(9.2%)	23.42	5.47	33.93	79.95	-0.242	30.10	chlo: 10, extr: 2, cyto: 1	Chloroplast
CrCML 22	03T010654	203	E(11.3%),F(10.8%),S(10.3%)	23.75	4.75	52.45	72.96	-0.467	38.92	nucl: 9, cyto: 2, extr: 2	Chloroplast
CrCML 23	04T011122	148	E(13.5%),D(12.8%),L(8.8%)	17.08	4.05	24.54	88.85	-0.420	32.43	cyto: 6, cyto_nucl: 6, chlo: 4, extr: 1	Cytoplasm
CrCML 24	04T011931	206	S(10.7%),A(9.7%),D(9.2%), G(9.2%)	22.30	4.62	36.41	71.55	-0.270	66.02	nucl: 7, mito: 4, chlo: 2	Chloroplast

CrCML 25	04T012182	163	L(13.5%),E(9.8%),A(9.2%)	18.29	4.53	42.13	91.66	-0.279	30.06	nucl_plas: 5.5, nucl: 5, plas: 4, cyto: 2, mito: 2	Chloroplast
CrCML 26	04T012874	84	E(15.5%),V(11.9%),L(8.3%)	9.87	4.38	59.01	92.62	-0.230	23.81	cyto: 5, extr: 5, nucl: 2, chlo: 1	Chloroplast
CrCML 27	05T014580	172	K(11.6%),S(10.5%),E(9.3%), G(9.3%)	19.08	5.18	26.33	58.37	-0.505	47.09	cyto: 7, nucl: 3, chlo: 2, mito: 2	Nucleus
CrCML 28	05T014903	145	E(11.0%),L(10.3%),D(9.0%)	16.53	4.86	31.69	84.76	-0.403	35.86	nucl: 4, cyto: 3, plas: 2, chlo: 1, mito: 1, extr: 1, cysk: 1	Chloroplast
CrCML 29	05T015286	160	L(13.8%),A(8.8%),G(8.8%)	17.49	4.41	27.70	95.75	-0.022	40.00	plas: 5, nucl_plas: 4.5, cyto: 4, nucl: 2, chlo: 1, mito: 1	Chloroplast
CrCML 30	05T015406	224	E(12.1%),L(9.8%),K(9.8%)	25.17	4.83	44.01	88.75	-0.214	50.00	chlo: 9, extr: 3, nucl: 1	Cytoplasm
CrCML 31	05T017030	160	L(13.8%),A(9.4%),D(8.8%), G(8.8%)	17.59	4.30	32.93	90.31	0.057	42.50	chlo: 10, mito: 2, nucl: 1	Chloroplast
CrCML 32	06T018151	159	L(15.1%),D(10.7%),E(10.7%)	18.21	4.31	46.05	86.42	-0.359	43.40	nucl: 5, cyto: 5, chlo: 2, mito: 1	Cytoplasm
CrCML 33	06T018267	157	L(17.2%),E(12.1%),G(10.2%)	16.96	4.10	25.21	108.09	-0.061	33.76	cyto: 10.5, cyto_E.R.: 6.33333, E.R._vacu: 1.33333	Nucleus
CrCML 34	06T018865	84	D(11.9%),E(10.7%),A(9.5%)	9.31	4.21	20.60	67.38	-0.568	26.19	nucl: 5, cyto: 3, mito: 3, chlo: 1, plas: 1	Mitochondrion
CrCML 35	06T019154	98	G(9.2%),A(8.2%),K(8.2%)	11.20	8.79	20.00	81.63	-0.587	61.22	mito: 8.5, chlo_mito: 6, chlo: 2.5, nucl: 1.5,	Chloroplast

										cyto_nucl: 1.5	
CrCML 36	08T022893	150	D(12.7%),G(10.7%),E(10.0%)	16.99	4.34	26.75	72.07	-0.516	29.33	nucl: 4, chlo: 3, mito: 3, cyto: 2, extr: 2	Cytoplasm
CrCML 37	09T023581	141	E(14.9%),L(12.1%),G(9.9%)	16.14	4.34	46.10	75.39	-0.365	29.08	nucl: 6, chlo: 4, cyto: 2, mito: 1	Chloroplast
CrCML 38	09T025115	218	D(9.6%),L(9.6%),I(8.7%)	24.88	4.74	41.15	88.03	-0.259	50.00	chlo: 12, mito: 1	Nucleus
CrCML 39	10T025518	191	S(12.0%),E(11.5%),D(8.9%)	21.41	4.58	46.26	69.37	-0.468	46.07	chlo: 7, mito: 5, nucl: 2	Nucleus
CrCML 40	10T026298	149	D(11.4%),L(9.4%),E(7.4%)	16.89	4.70	34.32	80.54	-0.436	59.06	cyto: 9, cyto_nucl: 8, nucl: 3	Cytoplasm
CrCML 41	10T026655	190	S(12.6%),D(10.5%),L(10.5%)	21.90	4.77	51.14	70.32	-0.670	61.05	mito: 7.5, chlo_mito: 5.5, nucl: 4, chlo: 2.5	Chloroplast
CrCML 42	10T027366	165	E(11.5%),F(9.1%),V(8.5%)	19.30	4.82	45.76	83.15	-0.259	24.85	extr: 4, vacu: 3, E.R.: 3, golg: 2, chlo: 1	Chloroplast
CrCML 43	11T028665	210	S(12.9%),K(10.0%),G(8.1%), L(8.1%)	23.37	7.63	35.58	78.86	-0.304	47.14	nucl: 11, cyto: 3	Nucleus
CrCML 44	11T028666	84	A(10.7%),D(10.7%),E(10.7%)	9.31	4.37	14.27	74.40	-0.425	35.71	cyto: 8, nucl: 2, mito: 2, chlo: 1	Peroxisome

MW: molecular weight; PI: isoelectric point; II: instability index; AI: aliphatic index; GRAVY: grand average of hydropathicity. The molecular weight and isoelectric points of predicted CrCaMs/CrCMLs were detected using the ExPASy proteomics server (https://web.expasy.org/protparam/). The TMHMM Server 2.0 program (http://www.cbs.dtu.dk/services/TMHMM/) and the Protein Fold Recognition Server tool (PHYRE², http://www.sbg.bio.ic.ac.uk/phyre2/html/page.cgi?id= index) were used to predict the transmembrane helices and the 3D prediction of CrCaMs/CrCMLs. For the subcellular localization prediction, the online program WoLF_PSORT (https://www.genscript.com/wolf-psort.html) were used.

2.2. The Genes' Localization and Analysis of the CrCaM/CrCML Genes Structure

Because the *CrCaM/CrCML* genes were named based on their chromosomal locations, the seven *CrCaM*s and 44 *CrCML*s were distributed on the eleven *C. rosea* chromosomes orderly (Figure 1). Overall, three *CrCaM*s (*CrCaM2*, *CrCaM3*, and *CrCaM4*) were located on chromosome 04, and *CrCaM1*, *CrCaM5*, *CrCaM6*, and *CrCaM7* were located on chromosomes 03, 06, 07, and 11, respectively. Chromosomes 01, 03, and 05 held more *CrCML*s (more than or equal to five members), chromosomes 02, 04, and 10 each contained four *CrCML* genes, chromosome 09 contained three

CrCML genes, and chromosomes 06 and 11 each contained two *CrCML* genes. Chromosome 08 contained only one *CrCML* gene (*CrCML36*).

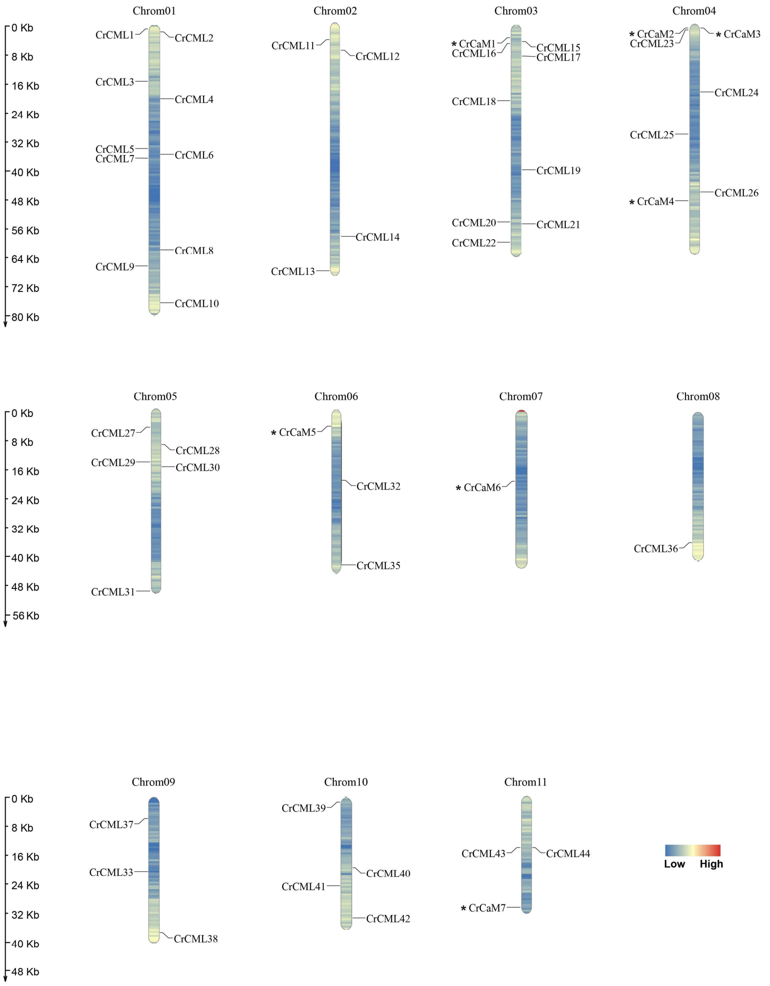

Figure 1. Locations of the 51 *CrCaMs*/*CrCMLs* on eleven chromosomes of *C. rosea*.

Many plant genomes undergo duplication and expansion events that would, in turn, lead to an increase in the number of functional response genes and the overall size of some specific families or generate multiple paralogs of some genes, resulting in multiple versions of similar proteins within an organism [40]. The gene duplication events also could be considered as important mechanisms for plant adaptive evolution at the genome level [41]. In this study, there were only two tandem duplication events (*CrCaM2*/*CrCaM3*, *CrCML43*/*CrCML44*) in the *CrCaM*/*CrCML* superfamily and fourteen segmental duplication events in *CrCML* subfamily (Table 2, Figure 2). The selection pressure imposed on the *CrCaM*/*CrCML* genes was assessed by calculating the ratio of non-synonymous (Ka) to synonymous (Ks) substitution values. We found that some of *CrCML* genes were under evolutionary pressure, with a Ka/Ks ratio ranging from 0.0111528 (*CrCaM5*/*CrCaM7*) to 0.370378 (*CrCML14*/*CrCML21*) (Table 2). The Ka/Ks values of the gene pairs were all considerably lower than 1.0, which suggested that these gene pairs were primarily selected for purification during the evolutionary process with limited functional divergence after duplication.

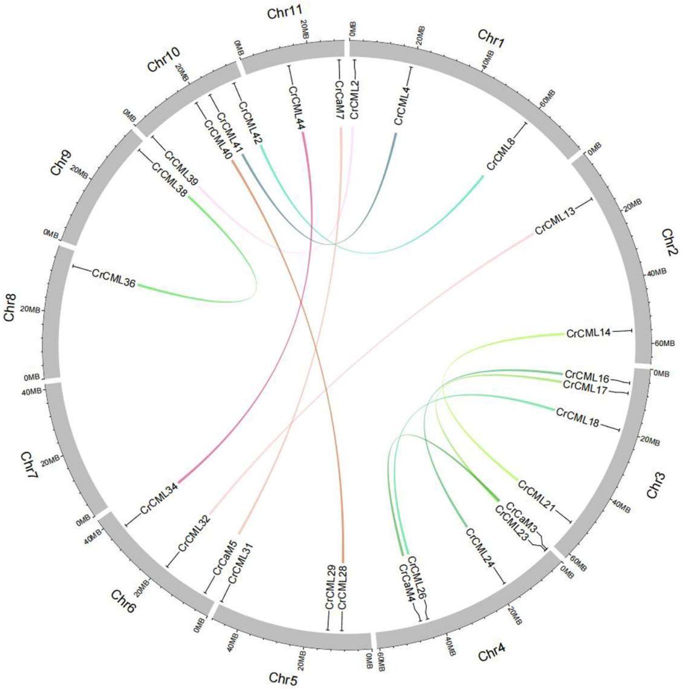

Figure 2. The distribution of segmental duplication of *CrCaMs*/*CrCMLs* in *C. rosea* chromosomes.

Table 2. Ka/Ks analysis and duplicated type calculation for *CrCaM* and *CrCML* genes.

Duplicated pair	Duplicate Type	Ka	Ks	Ka/Ks	P-Value(Fisher)	Positive Selection
CrCaM3-CrCaM4	Segmental	0.12532	0.542019	0.231209	6.07E-09	No
CrCaM5-CrCaM7	Segmental	0.00565853	0.507362	0.0111528	7.70E-24	No
CrCML2-CrCML39	Segmental	0.224798	1.46238	0.153721	4.27E-20	No
CrCML4-CrCML41	Segmental	0.147676	0.735966	0.200656	3.32E-14	No
CrCML8-CrCML42	Segmental	0.280668	0.761875	0.368392	5.48E-06	No
CrCML13-CrCML32	Segmental	0.200534	0.803216	0.249664	1.16E-08	No
CrCML14-CrCML21	Segmental	0.199284	0.538055	0.370378	1.25E-06	No
CrCML16-CrCML24	Segmental	0.250644	0.787603	0.318237	3.62E-10	No
CrCML17-CrCML23	Segmental	0.157841	0.707805	0.223001	2.98E-10	No
CrCML18-CrCML26	Segmental	0.137486	0.583507	0.235619	1.30E-08	No
CrCML28-CrCML40	Segmental	0.0930564	0.609897	0.152577	2.73E-13	No

CrCML29-CrCML31	Segmental	0.0905119	0.792094	0.114269	8.83E-20	No
CrCML34-CrCML44	Segmental	0.0645313	0.529471	0.121879	1.74E-08	No
CrCML36-CrCML38	Segmental	0.112235	1.05912	0.105971	1.19E-19	No
CrCaM2-CrCaM3	Tandem	\	\	\	\	\
CrCML43-CrCML44	Tandem	\	\	\	\	\

Furthermore, we analyzed the gene structures of the *CrCaM*/*CrCML* genes by comparing their coding sequences with their corresponding genomic DNA sequences (Figure 3). Generally speaking, the *CrCaM*s had more complicated gene structures than the *CrCML*s. Seven *CrCaM*s all had one to three introns, while only *CrCML6*, *CrCML17*, *CrCML18*, *CrCML19*, *CrCML23*, *CrCML26*, and *CrCML43* had introns. Among them, *CrCML26* and *CrCML43* contained only one intron, *CrCML17*, *CrCML18*, *CrCML19*; *CrCML23* contained three introns; and *CrCML6* contained five introns. Most of the *CrCML*s contained no introns. Obviously, the gene structure of the *CrCML*s was also relatively simple, which indicated their transcription and subsequent translation might be rapidly activated under different stress challenges because of the formation of mature mRNA of the *CrCML*s reduces the steps for the elimination of introns, thus shortening the response time. This further fortified the necessary functions of *CrCML*s in environmental stress responses.

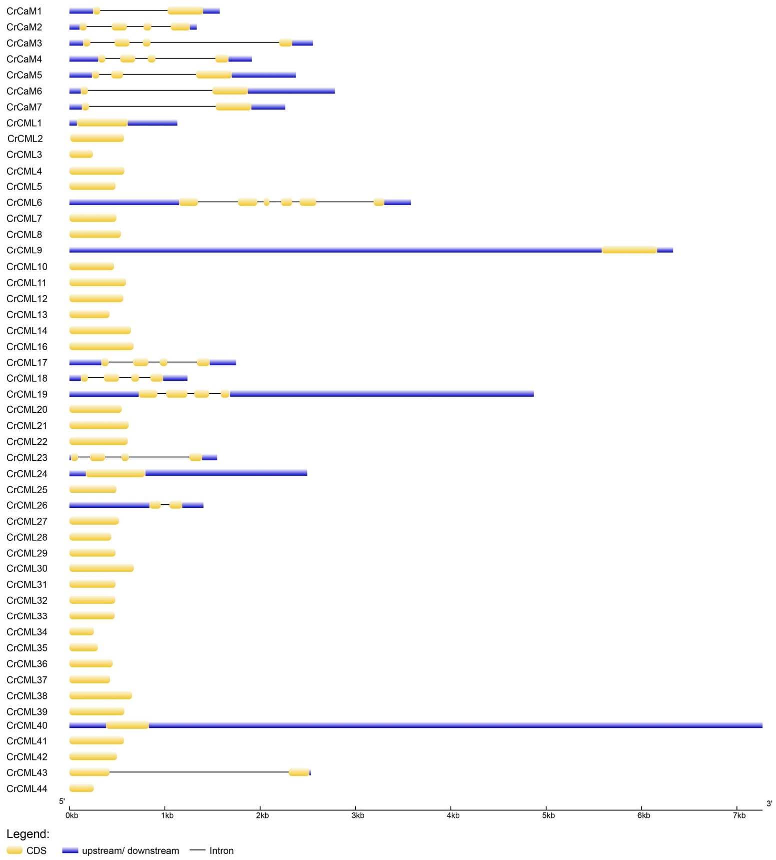

Figure 3. Exon-intron structures of the *CrCaMs*/*CrCMLs* predicted using the Gene Structure Display Server (GSDS, http://gsds.cbi.pku.edu.cn/).

doi:10.20944/preprints202410.0293.v1

2.3. The Conserved Motifs of Proteins and Phylogenetic Analysis

The CrCaM/CrCML conserved motifs were also demonstrated by the MEME analysis, and ten distinct motifs were identified (Figure 4). Motif 1 represented the typical EF-hand, and it was present in all CrCaMs with four repetitions. Most of the CrCMLs (23 of 44 CrCMLs) also contained four EF-hand motifs, while their conservativeness was inferior to that in the CrCaMs. In some CrCMLs (CrCML4, CrCML8, CrCML16, CrCML28, CrCML30, CrCML37, CrCML40, CrCML41, and CrCML42), motifs 2, 4, 7, and10 replaced the EF-hand motif, which might indicate that these CrCMLs are more diverse than the CaM proteins. Therefore, it also further inferred the complicated and changeable functions of the CrCML protein members.

Figure 4. Structural analysis of the CrCaM/CrCML proteins. The conserved motifs of each group identified by the MEME web server. Different motifs are represented by different colored boxes, and the motif sequences are provided at the bottom.

We first aligned the CrCaM/CrCML proteins to each other and performed their phylogenetic analysis (Figure 5). Undoubtedly, the seven CrCaMs were clustered into a small subgroup with a close evolutionary trend as CrCML16, CrCML17, CrCML18, CrCML23, and CrCML24. The CrCML10 seemed to be unique, and CrCML3, CrCML6, CrCML19, and CrCML35 also formed a relatively

doi:10.20944/preprints202410.0293.v1

independent cluster compared to other CrCaM/CrCML proteins. Overall, the CrCaM proteins were highly conserved, and half of the CrCMLs had high levels of similarity within protein pairs (over 90%, eleven pairs) that was probably generated by gene duplication.

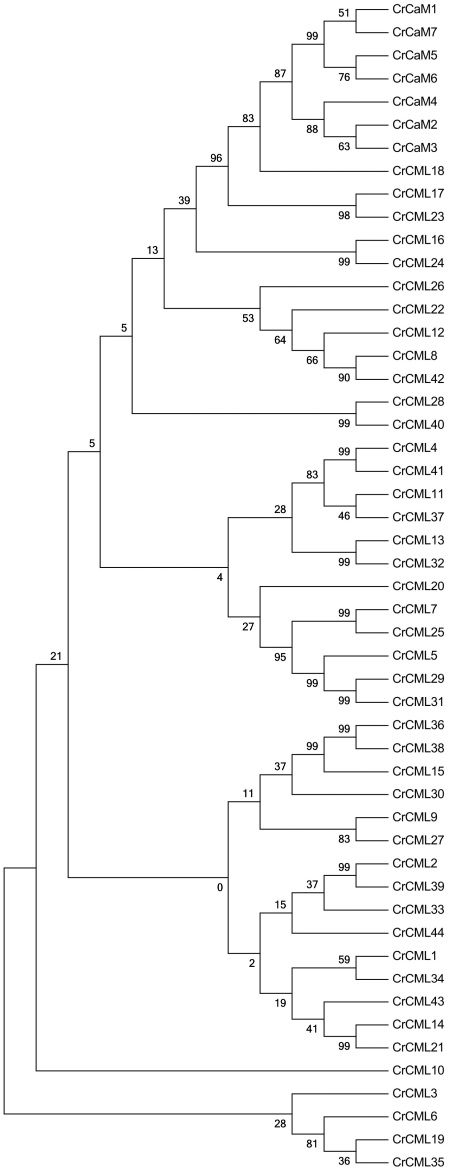

Figure 5. The phylogenetic tree of the CrCaMs/CrCMLs constructed using MEGA-X. The three major groups are marked with different color backgrounds.

To characterize the phylogenetic relationships of all of the CrCaM/CrCML proteins with similar members in the other species, we also inferred the phylogenetic relationships of the CaM/CMLs among *C. rosea*, rice, and Arabidopsis using the protein sequences of 57 AtCaM/AtCMLs, 37 OsCaM/OsCMLs, and 51 CrCaM/CrCMLs into seven cluster groups (containing 49, 23, 51, 13, 2, and 5 members in each group) (Figure 6). These groups were designated as I to VI, containing 13, 11, 19, 5, 1, and 2 CrCaM/CrCML proteins, respectively. Overall, the CrCaMs showed relatively high levels of similarity with those CaMs of other species, and they were highly conserved. The CMLs demonstrated relatively higher variability and diversity than CaMs. This was also consistent with the conserved motifs' analysis by MEME (Figure 4).

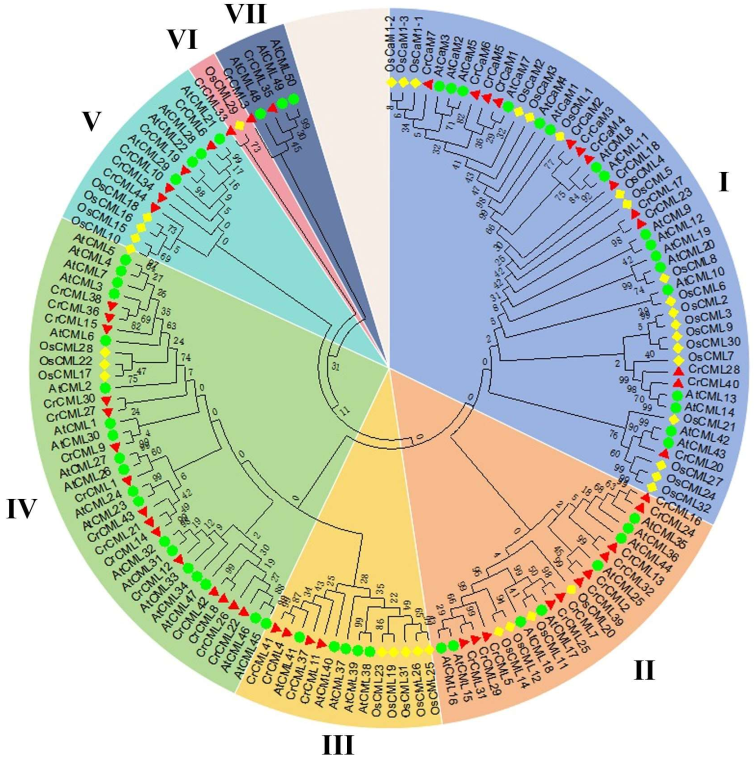

Figure 6. Phylogenetic relationships of the 51 CrCaMs/CrCMLs from *C. rosea*, 57 AtCaMs/AtCMLs from *Arabidopsis thaliana*, and 37 OsCaMs/OsCMLs from *Oryza sativa*. The amino acid sequences of these 145 CaMs/CMLs from the three plant species were compared with a ClustalW alignment, and the phylogenetic tree was constructed in MEGA X using the neighbor-joining method with 1000 bootstrap repetitions. The different branch colors represent different subgroups.

2.4. Abiotic Stress-Related Cis-Regulatory Elements (CEs) in the CrCaM/CrCML Promoters

To gain further insights into the regulatory mechanisms of *CrCaMs/CrCMLs* responding to environmental stresses and developmental signals, the promoter features of the *CrCaMs/CrCMLs* were systematically identified with different CE categories. Phytohormone and stress responses *cis*-regulatory elements in the promoter regions of the 51 *CrCaMs/CrCMLs* genes were predicted (Figure 7).

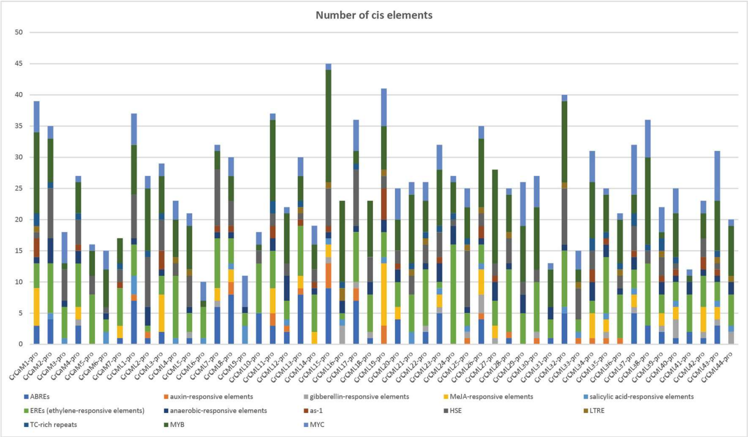

A

doi:10.20944/preprints202410.0293.v1

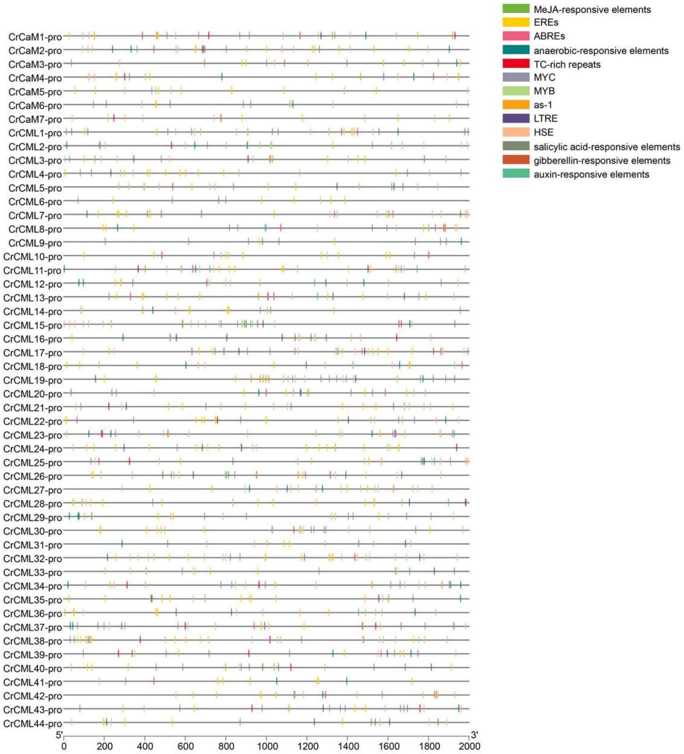

B

Figure 7. Statistics for the predicted *cis*-regulatory elements in the *CrCaMs*/*CrCMLs* promoters (ATG upstream 2000). (A) Summaries of the thirteen *cis*-regulatory elements in the 51 *CrCaMs*/*CrCMLs* promoter regions. (B) Distribution of these *cis*-regulatory elements in the 51 *CrCaMs*/*CrCMLs* promoter regions. The elements are represented by different symbols. The scale bar represents 200 bp.

The results revealed that the CEs associated with phytohormone responses, including abscisic acid (ABREs), auxin (auxin-responsive elements), gibberellin (gibberellin-responsive elements), methyl jasmonate (MeJA-responsive elements), salicylic acid (salicylic acid-responsive elements), and ethylene (EREs), existed extensively in most of the *CrCaMs*/*CrCML* promoter regions. Some adversity-related CEs, such as anaerobic-responsive elements, low temperature, heat stress elements (HSE), and defense and stress-related elements (TC-rich repeats), also occurred widely in the promoter regions of the *CrCaMs*/*CrCMLs*. The *CrCaMs* and *CrCMLs* had the same or different CEs, indicating that these genes may be regulated in response to stress sometimes simultaneously, or that these genes respond to adverse external environments especially.

2.5. Tissue- and Habitat-Specific Expression Profiles of the CrCaMs/CrCMLs

The expression patterns of the *CrCaMs*/*CrCMLs* were detected first with a RNA sequencing analysis concerned with tissue specific patterns, and the purpose was to confirm the real transcripts of the *CrCaMs*/*CrCMLs* that might be involved in *C. rosea* growth and development. The expression levels of the *CrCaMs*/*CrCMLs* in five different tissues (including the roots, vines, leaves, flower buds, and young fruit) were calculated and displayed using a heatmap (Figure 8A) according to the RNA-seq data (Table S3). Nearly half of the *CrCaMs*/*CrCMLs* showed relatively higher expression levels in both the roots and flower buds than that in vines, leaves, and young fruit, with log2-transformed FPKM values greater than or equal to two (Figure 8A). In young vine tissues of *C. rosea* plants, only *CrCaM5*, *CrCaM7*, *CrCML10*, *CrCML29*, and *CrCML41* presented relatively high expression levels; while in leaf tissues, only *CrCML9*, *CrCML24*, *CrCML31*, and *CrCML43* were relatively high-expressed. In young fruit tissues of adult *C. rosea*, the global expression levels of all of the *CrCaMs*/*CrCMLs* showed relatively lower levels, and only *CrCML14* and *CrCML42* were expressed in the fruit at high levels, indicating that these two genes may be involved in the reproduction of *C. rosea* plants.

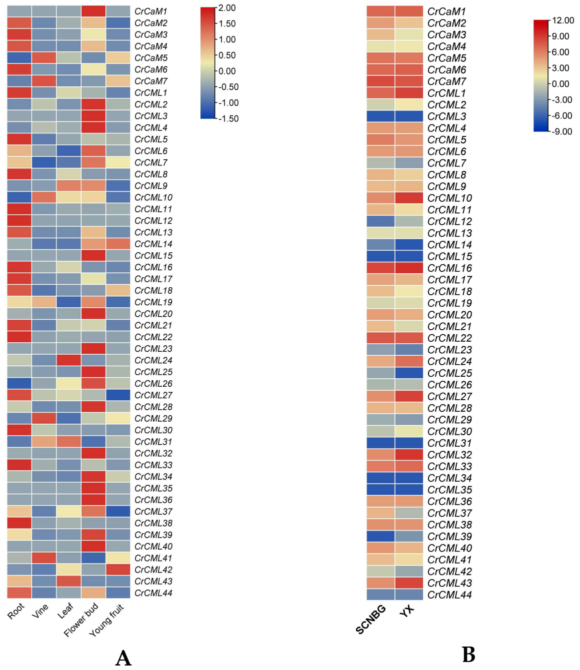

Figure 8. Heatmaps showing (A) the expression levels of the *CrCaM*s/*CrCML*s in the root, stem, leaf, flower bud, and young fruit of *C. rosea* plants and (B) the expression differences of the *CrCaM*s/*CrCML*s in mature *C. rosea* leaves planted in the South China National Botanical Garden (SCNBG) and in Yongxing (YX) Island.

Canavalia rosea is a typical tropical leguminous halophyte, and this species shows great growth advantages on tropical coral islands and reefs with excellent tolerance to heat, drought, high salinity/alkalinity, strong sun light, and high ultraviolet radiation. Halophytes are plants that can complete their life cycles under very high salt concentrations and even benefit from this special habitat [42]. It has been reported that the expression of halophyte-derived genes improves the tolerance of transgenic plants in response to various stresses [43,44]. In this regard, we performed a gene expression analysis of two mature leaf samples gathered from SCNBG (optimal habitat) and YX Island (special habitat) (Figure 8B). Except for five *CrCaM*/*CrCML* genes, including *CrCML3*, *CrCML15*, *CrCML31*, *CrCML34*, and *CrCML35*, the others all showed more or less transcripts both in the SCNBG and the YX tissue samples. More obviously, several genes showed relatively higher expression levels in the YX sample, including *CrCML1*, *CrCML10*, *CrCML24*, *CrCML27*, *CrCML32*, and *CrCML43*, and only *CrCaM2*, *CrCaM3*, *CrCML11*, *CrCML18*, *CrCML21*, *CrCML37*, and *CrCML41* presented slightly lower expression levels in the YX sample than that in the SCNBG sample. This result indicated that some *CrCaM*s/*CrCML*s might play positive protective roles in *C. rosea*’s adaptation to coral reef habitats. The RNA-sequence data of the *CrCaM*s/*CrCML*s are listed in Table S3.

2.6. Expression Profile of the CrCaM/CrCML Genes in Response to Abiotic Stress

A promoter analysis of the *CrCaM*/*CrCML* genes indicated that the transcriptional regulatory model of this gene family was diverse and member-specific. Plant *CaMs*/*CMLs* have been proven to be modulated by multiple environmental stressors, including heat, cold, salt, drought, or heavy metals [18–20], and some individual plant *CaM* or *CML* genes have been proven to mediate stress tolerances by modulating downstream co-factors [21–27] .

The *CaM* or *CML* genes isolated from special habitat plants that had heterologous transgenic experiments performed provided further evidence of their clear functions for environmental stress responses [25,28]. *Canavalia rosea* is a unique plant that is adapted to specialized habitats, thriving especially on coral reefs. This suggests that the species can withstand various environmental challenges, such as drought, high osmotic pressure, salinity/alkalinity, heat, and intense bright light or high ultraviolet radiation. Furthermore, whether the halophyte *C. rosea*’s *CaM*/*CML* genes can also function in multiple environmental conditions has also become an interesting research topic. To recognize the role of heat-related signaling responses in the regulation of *CrCaMs*/*CrCMLs*, an expression analysis was performed with plants treated with heat (42°C) using RNA-sequencing. Both in the root and in leaf samples, more than half of the *CrCaMs*/*CrCMLs* exhibited obvious expression alterations and were up- or down- regulated by heat challenge (Figure 9). In general, in both the root and leaf samples, a large proportion of the *CrCaMs*/*CrCMLs* showed decreased expression levels under heat stress. However, in two *C. rosea*'s tissues, several noticeably up-regulated *CrCaMs*/*CrCMLs* members raised concern, including *CrCaM2*, *CrCML7*, *CrCML29*, *CrCML32*, and *CrCML43* in roots and *CrCML3*, *CrCML4*, *CrCML8*, *CrCML9*, *CrCML24*, *CrCML25*, and *CrCML39* in leaves. This suggested that the above *CrCaM*/*CrCML* members were genes with different but unique potential biological functions in the heat responses of *C. rosea* plants.

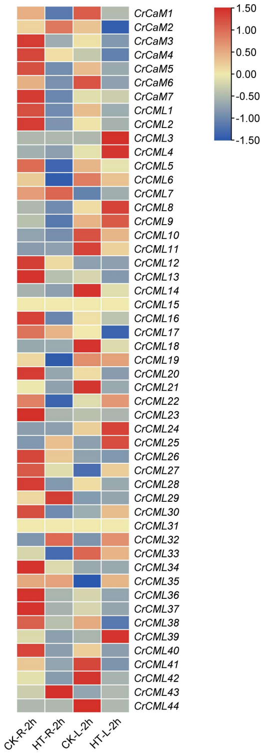

Figure 9. Heatmaps showing the expression levels of the RNA-Seq data for the *CrCaMs*/*CrCMLs* in the root and leaf samples captured from the heat-shock-treated *C. rosea* seedlings. The expression level of each gene is shown in values of log2 (FPKM+1). Red denotes high expression levels, and green denotes low expression levels. Data normalization was performed on the website of Oebiotech Cloud.

We further analyzed the expression of all family members in *C. rosea* seedling plants subjected to high salinity, alkaline, and high osmotic (mimic drought) stresses. Overall, we noticed that the modulation of specific *CrCaMs*/*CrCMLs* showed completely different expression patterns, either in roots (Figure 10A) or in leaves (Figure 10B). We also reconfirmed the expression patterns of some candidate *CrCaMs*/*CrCMLs* with qRT-PCR, and the results also demonstrated that heat, high salinity, alkaline, osmotic stress, and oxidative stress could rapidly induce the transcript changes in the roots, stems, and leaves of *C. rosea* plants (Figure 11). In summary, under heat stress, the *CrCaMs*/*CrCMLs* exhibited more pronounced expression changes in the roots compared to the stems and leaves. However, in response to other abiotic stresses, such as high salinity/alkalinity, high osmotic pressure, and oxidative stress, a larger number of *CrCaMs*/*CrCMLs* showed greater expression changes in the leaves, particularly after prolonged stress exposure (L-48 h), compared to the roots (Figures 10 and 11). Notably, several members, including *CrCaM2*, *CrCaM3*, and *CrCaM4*, exhibited substantial expression changes under most stress challenges, making them particularly intriguing for further study. Further identification of stress-regulated expressed patterns about the *CrCaMs*/*CrCMLs* can provide more information for the ecological suitability for extreme adversity of *C. rosea* plants.

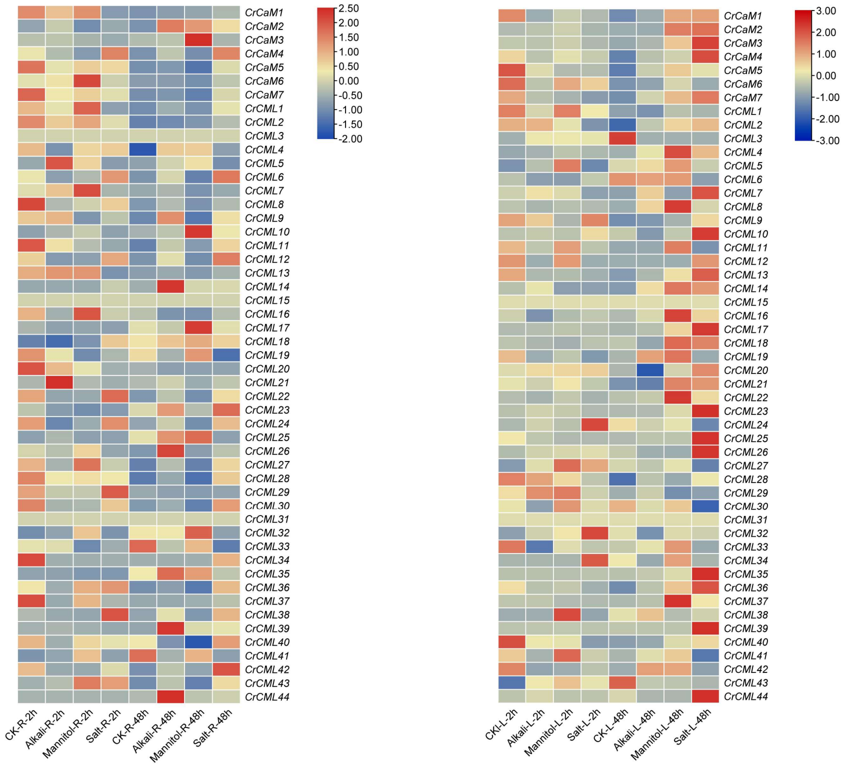

A **B**

Figure 10. Heatmaps showing the expression changes of the RNA-Seq data for the *CrCaM*s/*CrCML*s under high salinity, alkaline, and high osmosis stresses. The expression levels of each gene are shown in values of log2 (FPKM+1). The expression differences of 51 *CrCaM*s/*CrCML*s in the root (A) and leaf (B) after the 2 h and 48 h abiotic stress challenge. Data normalization was performed on the website of Oebiotech Cloud.

doi:10.20944/preprints202410.0293.v1

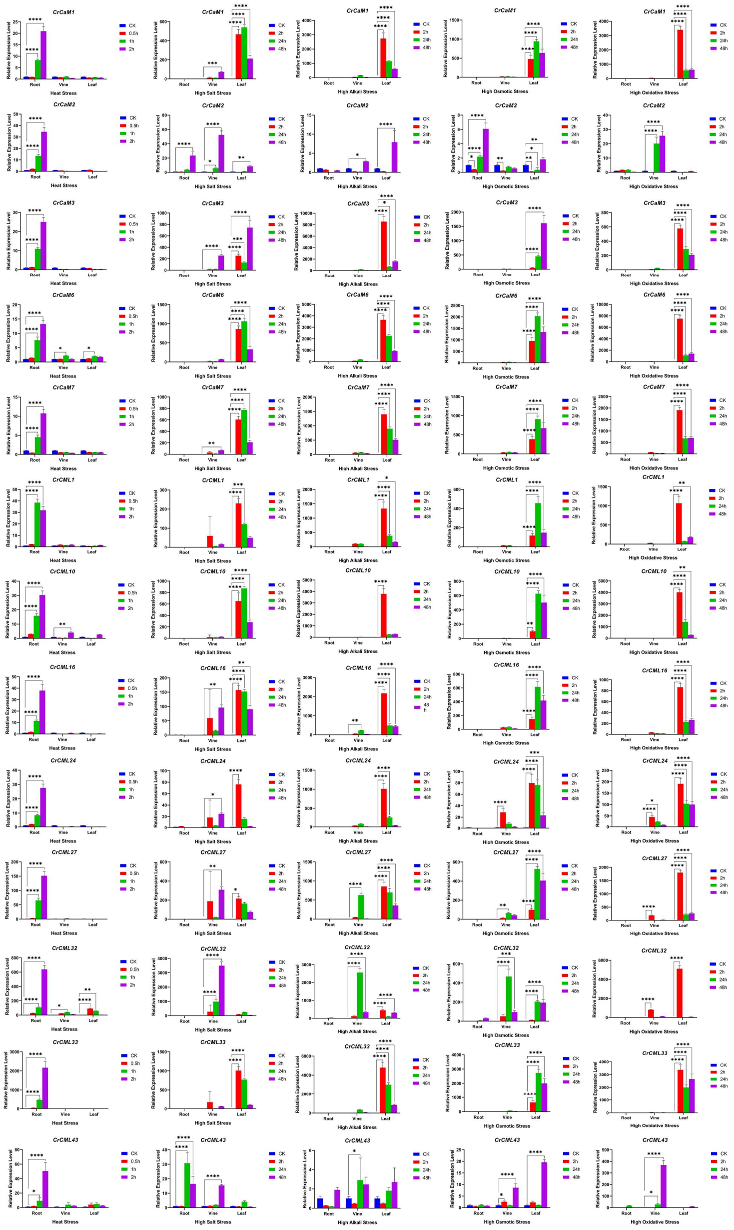

Figure 11. Quantitative RT-PCR detection of the expression levels of the thirteen *CrCaMs*/*CrCMLs* responding to different abiotic stresses, including heat (45°C), high salt (600 mM NaCl), alkaline (150 mM $NaHCO_3$, pH 8.2), high osmotic stress (300 mM mannitol), and H_2O_2 (10 mM) oxidative stress. The relative expression values were calculated using the $2^{-\Delta Ct}$ method with the housekeeping gene, *CrEF-1α*, as a reference gene. The bars show the mean values ± SDs of n = 3–4 technical replicates.

2.7. Functional Characterization of the CrCaMs/CrCMLs in Yeast

To provide relevant biological significance combined with the *in silico* expression meta-analysis of the *CrCaMs*/*CrCMLs*, the initial functional identification of some *C. rosea CaM*/*CML* genes was investigated using the yeast heterogeneous expression system. In short, the cDNAs' open reading frames of *CrCaM1*, *CrCaM3*, *CrCaM6*, *CrCaM7* and *CrCML1*, *CrCML10*, *CrCML16*, *CrCML24*, *CrCML27*, *CrCML32*, and *CrCML33* were PCR cloned and inserted into the expression cassette of pYES2 under a galactose-induced promoter. The WT yeast was then transformed with recombinant CrCaMs/CrCMLs-pYES2 vectors, and stress tolerance tests were performed that included heat (52°C), high salinity (NaCl), alkaline ($NaHCO_3$), high osmotic challenge (sorbitol), and oxidative stress (H_2O_2).

doi:10.20944/preprints202410.0293.v1

To explore the role of *C. rosea CaM/CML* in the regulation of stress tolerance *in vivo*, the growth of yeast strains containing recombinant CrCaMs/CrCMLs-pYES2 vectors was first compared with control cells (transformed with empty vector pYES2) after a high-temperature challenge (52°C). The H_2O_2-sensitive mutant strain, *skn7Δ*, is also sensitive to heat, and the 52°C treatment for 15 min was nearly lethal for *skn7Δ*, while all the *CrCaM/CrCML* members improved the survival rate of the *skn7Δ* strain to varying degrees. In addition, under prolonged heat (52°C for 20 min), some of the *CrCaM/CrCML* genes even improved the growth status of *skn7Δ* better than the WT (Figure 12A). From this, we can conclude that in the single-cell yeast system, the heat damage was mitigated to different extents by an accumulation of CrCaM/CrCML proteins. Unexpectedly, the results indicated that the CrCaM/CrCML proteins did not seem to elevate the H_2O_2-tolerance of *skn7Δ* (Figure 12B), and this might imply another antioxidant signaling pathway by the calcium signals.

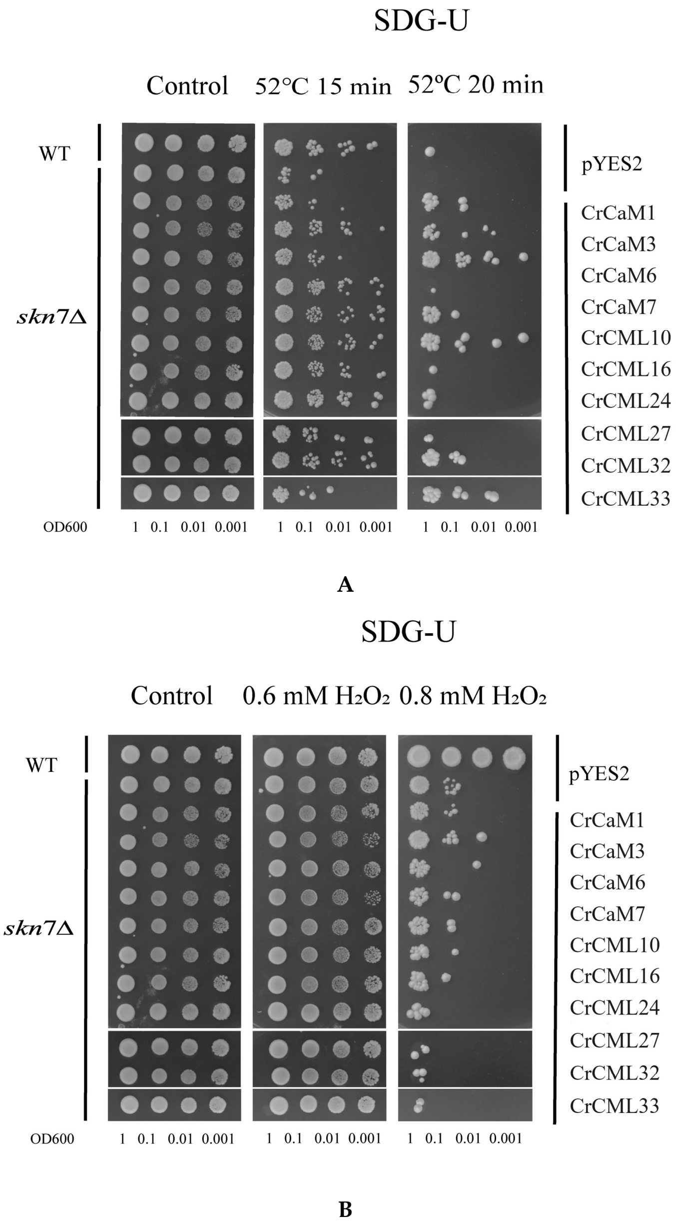

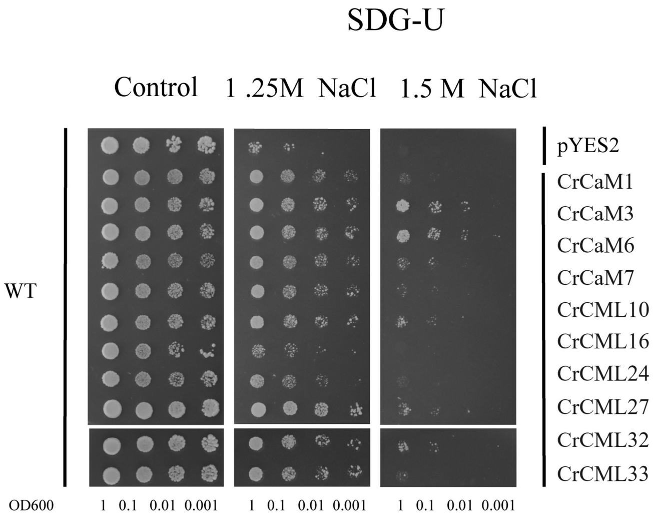
SDG-U
Control
1 .25M NaCl
1.5 M NaCl
WT
pYES2
CrCaM1
CrCaM3
CrCaM6
CrCaM7
CrCML10
CrCML16
CrCML24
CrCML27
CrCML32
CrCML33
OD600
1 0.1 0.01 0.001
1 0.1 0.01 0.001
1 0.1 0.01 0.001

C

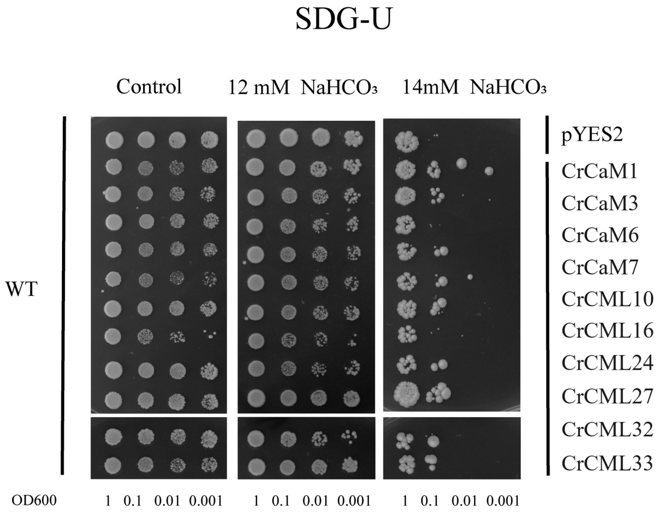
SDG-U
Control
12 mM NaHCO₃
14mM NaHCO₃
WT
pYES2
CrCaM1
CrCaM3
CrCaM6
CrCaM7
CrCML10
CrCML16
CrCML24
CrCML27
CrCML32
CrCML33
OD600
1 0.1 0.01 0.001
1 0.1 0.01 0.001
1 0.1 0.01 0.001

D

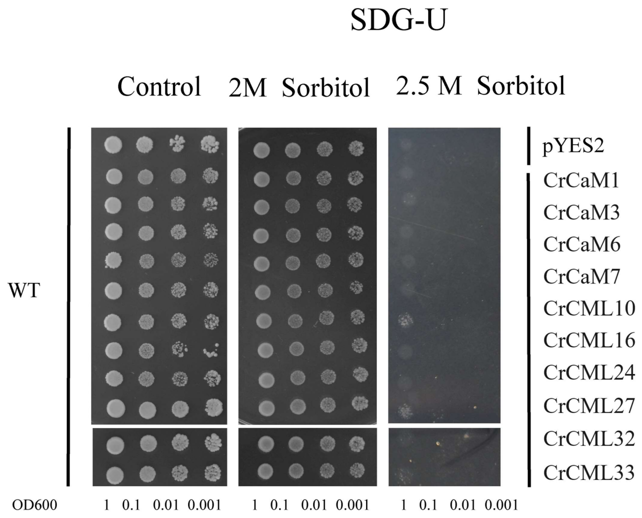
SDG-U
Control
2M Sorbitol
2.5 M Sorbitol
WT
pYES2
CrCaM1
CrCaM3
CrCaM6
CrCaM7
CrCML10
CrCML16
CrCML24
CrCML27
CrCML32
CrCML33
OD600
1 0.1 0.01 0.001
1 0.1 0.01 0.001
1 0.1 0.01 0.001

E

Figure 12. The functional confirmation in yeast strain WTs and *skn7Δ* by expressing ten *CrCaMs*/*CrCMLs*. Yeast cultures (WT: 52°C for 30 min for heat stress; *skn7Δ*: 52°C for 15 min for heat stress; or WT without challenges) were adjusted to OD600 = one, and 2 μL of serial dilutions (10-fold) were spotted on SDG-Ura medium plates supplied with specific challenge stressors. The plates were incubated for 2–5 days at 30°C. Functional identification of ten *CrCaMs*/*CrCMLs* in yeast using a heterologous expression assay. (A) The thermotolerance confirmation in the yeast mutant strain, *skn7Δ*; (B) H_2O_2 oxidative stress tolerance confirmation in the yeast mutant strain, *skn7Δ*; (C) high salinity tolerance confirmation in the WT yeast on NaCl-surplus SDG-Ura medium plates; (D) high alkaline tolerance confirmation in the WT yeast on $NaHCO_3$-surplus SDG-Ura medium plates; and (E) the high osmotic stress tolerance confirmation in the WT yeast on sorbitol-surplus SDG-Ura medium plates.

The plants' *CaMs* and *CMLs* were also involved in diverse cellular processes including signaling and other different abiotic stress responses [10]. We also detected the salt (Figure 12C), alkaline (Figure 12D), and high osmotic stress (Figure 12E) tolerance of WT yeast. The tested *CrCaM*/*CrCML* genes all improved the NaCl tolerance of yeast to different degrees, and *CrCaM3*, *CrCaM6*, and *CrCML27* appeared to possess the best tolerability. However, for alkalinity, it seemed that *CrCaM6* and *CrCML16* did not affect the alkali tolerance of yeast, while other genes all improved the alkali tolerance to varying degrees. As for high osmotic stress, it seemed that only *CrCML10* and *CrCML27* slightly elevated the osmotic tolerance of yeast. The above experiments were repeated at least three times.

3. Discussion

Calcium, a universal second messenger, plays a key role in the signal transduction process during plant growth, development, and the stress response [45]. Plants have evolved a series of physiological and biochemical mechanisms to cope with environmental and developmental stimuli. One of the most important ways is to recruit Ca^{2+} by proteins' EF-hand domains and then the Ca^{2+} acts as a second messenger in response to a given stimulus [46]. In this study, the *C. rosea* proteome was searched with the conserved EF-hand domain (PF13499), and the *CrCaM*/*CrCML* gene family was identified. The related evolutionary relationships, sequence features, and duplication events were also explored systematically.

Until now, at least four leguminous plants' *CaM* or *CML* gene families have been systematically identified at the genome-wide level, and these include *Lotus japonicus* (7 *LjCaMs* and 19 *LjCMLs*) [47], *Medicago truncatula* (50 *MtCMLs*) [48], *Glycine max* (soybean) (41 *GmCMLs*) [49], and *Phaseolus vulgaris* (common bean) (111 *PvCMLs*) [50]. These genes are all supposed to be involved in plant development according to RNA-seq assays with different tissues or organs, and some of them might also mediate abiotic or biotic stress responses [47,48]. On the whole, the numbers of *CaMs* in plants are basically below 10, while the numbers of *CMLs* in plants are up to dozens, even one hundred. A previous report had indicated that the varied gene number of plants' *CaM* or *CML* and in genomes might be dependent on evolutionary pressure, functional requirements, and complexities of the plant [9]. This combined with the gene structures of *CrCaMs* or *CrCMLs* (containing more introns in *CaMs* while less or no introns in *CMLs*) (Figure 3) allow us to propose that *CrCaMs* and *CrCMLs* might play different cellular and ecological roles associated with *C. rose*'s adaptation and the evolution of this species.

Some specific *CaM* or *CML* gene members have been systematically investigated via transgenic assays. For example, in the leguminous alfalfa plant, the overexpression of *Medicago sativa MsCML46* enhances transgenic tobacco's tolerance to freezing, drought, and salt stresses by improving the contents of osmotic regulatory solutes and antioxidant enzyme activity while decreasing reactive oxygen species (ROS) accumulations [23]. Another alfalfa (*Medicago truncatula*) *CML* gene, *MtCML42*, can prompt early flowering by up-regulating the flowering-time gene, *MtFTa1*, and mediating cold tolerance by affecting stress resistant gene expressions such as *MtABI5*, *MtCBF1*, and *MtCBF4* [51]. In crops, some *CaM* or *CML* genes have also been proven to possess positive regulating plant resistance. The *Cucumis melo CmCML13* can enhance the salt tolerance of transgenic Arabidopsis through reducing the shoot Na^+ content and also improving the drought resistance [22]. The ectopic expression of the finger millet (*Eleusine coracana*) CaM gene, *EcCaM*, confers improved drought and salinity tolerance in Arabidopsis by regulating ion leakage, the proline content, and the antioxidant capacity [24]. The potato (*Solanum tuberosum*) CaM gene, *StCaM2*, was induced by multiple abiotic stresses in potato tissues, and its overexpression in transgenic tobacco plants can enhance the tolerance to salinity and drought stress [27]. Conversely, the barley (*Hordeum vulgare*) CaM gene, *HvCaM1*, negatively regulates salt tolerance. Although its expression is significantly induced by long-term salt stress in barley tissues, the overexpression (OE) of *HvCaM1* in barley resulted in the reduced salt tolerance than *HvCaM1* knockdown (RNA interference) lines and the WT [21]. From this, we can conclude that for some specific *CaM* or *CML* genes, their biological functions might be unique, and even their expression is obviously induced under stress challenges. In addition, the functions are also possibly opposite, which suggests that further research regarding unknown plant *CaM* or *CML* genes might be quite a tough challenge.

Canavalia rosea is a highly resistant plant species distributed in special habitats, primarily in tropical or subtropical coastal saline regions [15]. Due to its strong vitality and enormous ecological landscape benefits for islands and reefs, this species has caused extensive concern in recent years. In this research, from the point of view of the phylogenetic analyses of *CrCaM*s and *CrCML*s, the protein structure prediction, the gene expression summary, and some transgenic assays with yeast, we expounded to comparative gene families and discussed the function of these genes for the ecological adaptation of *C. rosea*, as well as exploring and evaluating the possible values for future crop genetic improvements. In fact, there has been some exploratory research regarding the biological functions of *CaM* or *CML* genes from special habitat plants. The semi-mangrove *Millettia pinnata* showed excellent adaptation to the saline environment, and the salt-responsive CML gene, *MpCML40*, was induced by salt treatment in the *M. pinnata* plant. The *MpCML40* over-expressed transgenic Arabidopsis presented highly enhanced the seed germination rate and root length under salt and osmotic stresses, further clarifying the positive regulating roles of *MpCML40* in response to salt stress and potential application values for generating salt-tolerant crops [25]. *Paspalum vaginatum* O. Swartz is a typical seashore paspalum halophyte in tropical and subtropical coastal regions worldwide, and this species has exuberant vitality even under persistent high salinity/alkaline stressors. A *CML* gene from *P. vaginatum*, *PvCML9*, was highly expressed in *P. vaginatum* roots and stems, and over-expression of *PvCML9* in rice and paspalum led to reduced salt tolerance. Instead, down-regulating expression of this gene in paspalum showed increased salt tolerance [28]. *Nitraria sibirica* Pall. (*N. sibirica*) is a typical halophyte with strong adaptability to extreme saline-alkali and drought environments. Some of the *N. sibirica CaM*/*CML* genes showed considerably regulated expression patterns due to high salt challenges, and the overexpression of two *NsCML*s was found to mitigate H_2O_2 accumulation caused by abiotic stresses, thereby regulating ROS homeostasis and further indicating the possible molecular mechanisms of *NsCML*s-mediated abiotic stress tolerance in *N. sibirica* [32]. A precious woody species, *Phoebe bournei*, is a subtropical evergreen broad-leaved tree species. Now this species is faced with seriously threats to its survival due to habitat degradation, primarily due to contentious drought challenges. The *PbCaM*s/*PbCML*s might be related to the stress responses of *P. bournei*, and the overexpression of *PbCaM3*/*PbCML13* genes significantly increased the tolerance of yeast cells to drought stress [52].

Although the *CrCaM* and *CrCML* genes were evolutionary highly conserved, their biological functions might be unique. Heat, salt, high alkalinity, and drought are also major environmental challenges that limit plant growth and development in the special habitats of tropical islands or reefs, and we propose that *CrCaM* and *CrCML* genes might be recruited to cope with multiple stress challenges in the special habitats of *C. rosea* plants. In this study, we also cloned several *CrCaM* and *CrCML* genes and ectopically expressed them in yeast for a functional confirmation. Opposite of our expectation for heat tolerance, all of the detected *CrCaM*s and *CrCML*s improved the heat tolerance of the H_2O_2-sensitive mutant yeast strain *skn7Δ*, while the H_2O_2 tolerance of *skn7Δ* was nearly unaffected (Figure 11A,B). Similarly, the high salinity and alkaline tolerance of the WT yeast strain was also changed (up- or down- regulated) by the expression of *CrCaM*s and *CrCML*s (Figure 11C,D), while the high osmotic stress tolerance remained largely unchanged ((Figure 11E). This is quite different from other *C. rosea* molecular chaperone genes, such as *CrLEA*s/*ASR*s [33] or *CrCYSTM*s [39]. From this we can also conclude that the functions of specific plant *CaM* or *CML* genes are unique and require further individual investigations.

In summary, this study identified the *C. rosea CrCaM* and *CrCML* gene family, consisting of seven novel *CaM* members and 44 *CML* members. Sequence analysis showed that of all CrCaM and CrCML proteins contained the EF-hand domain (PF13499). We also conducted RNA-seq analysis to examine the gene and promoter sequences of the *CrCaM* and *CrCML* family, aiming to understand their biological functions under abiotic stresses, as well as the natural ecological adaptability of *C. rosea* plants to tropical and subtropical coastal areas. Overexpression of certain *CrCaM* and *CrCML* genes in yeast resulted in altered tolerance to heat, salt, and high alkalinity stress. These findings offer comprehensive insights into the *C. rosea CrCaM* and *CrCML* gene family, paving the way for further functional studies on plant CaMs/CMLs. Additionally, these results will support further research on the role of CrCaMs/CrCMLs as protective molecules and mediators of responses to environmental conditions and to internal developmental signals.

4. Materials and Methods

4.1. Plant Materials and Stress Treatments

The *C. rosea* seedlings were cultivated with seeds gathered from the coastal regions of Hainan Province, China. The plant growth conditions were maintained in an artificial greenhouse system (22°C with a photoperiod of 16 h light/8 h darkness) in the South China National Botanical Garden (SCNBG, 23°18′76″ N, 113°37′02″ E). The tissues of *C. rosea* plants were also captured from Yongxing Island (YX, 16°83′93″ N, 112°34′00″ E) and the South China National Botanical Garden (SCNBG) for gene expression detection. One-month old *C. rosea* seedlings were used for the different abiotic stress treatments. In brief, the seedling roots were soaked in 600 mM NaCl, 150 mM $NaHCO_3$ (pH 8.2), 300 mM mannitol, a 45°C pre-warmed 1/2 Hoagland solution, and 10 mM H_2O_2 for high salinity, alkaline, high osmotic, heat stress, and oxidative stress treatments, respectively. Plant tissues were collected at different time points (2 and 48 h for the RNA-seq or qRT-PCR). Three independent biological replicates were used.

4.2. Identification and Evolutionary Analyses of the CrCaM/CrCML Family in C. rosea

All of the collected genome sequencing data was submitted to GenBank (Accession No.: JACXSB000000000, will be released on September 16, 2024). The Pfam ID (EF-hand domain pair, PF13499) was used to search for the CrCaM/CrCML family members, and putative sequences of the CrCaM/CrCML proteins were identified and submitted to the National Center of Biotechnology Information (NCBI) Conserved Domain Database (https://www.ncbi.nlm.nih.gov/Structure/cdd/wrpsb.cgi, accessed on 10 April 2024) to confirm the presence of the EF-hand domain. The sequence information is summarized in Table S1.

The amino acid sequences of CrCaMs/CrCMLs were aligned using ClustalW software by MEGA-X software, and a phylogenetic tree was constructed using the neighbor-joining (NJ) phylogenetic method with 1000 bootstrap replicates. The CrCaMs/CrCMLs were also compared with those from other plant species using a multiple sequence alignment conducted using ClustalX software. The CaM/CML protein sequences of Arabidopsis (7 AtCaMs and 50 AtCMLs) [12] and rice (5 OsCaMs and 32 OsCMLs) [13] were downloaded from TAIR and RAP-DB (https://rapdb.dna.affrc.go.jp/, accessed on 10 April 2024), respectively. The amino acid sequences of these three species' CaMs/CMLs were used to construct the phylogenetic tree.

4.3. Chromosomal Location, Ka/Ks Calculation of the CrCaM/CrCML Genes, and Conserved Motifs of the Proteins

All of the *CrCaM*/*CrCML* family members were mapped to the chromosomes and scaffolds of *C. rosea* based on their physical location information. The genes' localization was visualized using MG2C 2.1 (http://mg2c.iask.in/mg2c_v2.1/, accessed on 10 April 2024) and Adobe Illustrator. The synonymous and non-synonymous substitution rates (Ks and Ka, respectively) and the probability (P-value) of Fisher's exact test of neutrality were calculated to explore the selective pressures on the duplication of *CrCaMs*/*CrCMLs* based on all nucleotide sequences using the Nei-Gojobori model with 1000 bootstrap replicates [53]. The gene duplication events were analyzed using the Multiple Collinearity Scan toolkit (MCScanX, http://chibba.pgml.uga.edu/mcscan2/, accessed on 10 April 2024) with default parameters, and tandem duplications were identified manually (Table 2). The gene structures, including the intron-exon patterns and the 5′ and 3′ untranslated region (UTR) of the *CrCaM*/*CrCML* genes, were displayed through the GSDS2.0 server (http://gsds.gao-lab.org, accessed on 10 April 2024).

doi:10.20944/preprints202410.0293.v1

To further investigate the features of the CrCaMs/CrCML proteins, conserved motifs were analyzed using the MEME program (Multiple Em for Motif Elicitation, http://meme-suite.org/index.html, accessed on 10 April 2024) with the following parameters: motif number was set to 10, classic motif discovery mode, and any number of repetitions.

4.4. Cis-Regulatory Element Analysis of the CrCaM/CrCML Promoters

The predicted *cis*-regulatory elements (CEs) were scanned using the PlantCARE program (http://bioinformatics.psb.ugent.be/webtools/plantcare/html/, accessed on 10 April 2024) by searching for the promoter regions (2000 bp upstream from the translation start site ATG) of all the *CrCaMs*/*CrCMLs*. These CEs were classified into hormone-specific (ABREs, auxin-responsive elements, gibberellin-responsive elements, MeJA-responsive elements, salicylic acid-responsive elements, and EREs) and environmental or development responsive (anaerobic-responsive elements, as-1, HSE, LTRE, TC-rich repeats, MYB, and MYC), and are summarized in Table S2. The CE analysis results were visualized and mapped to the *CrCaM*/*CrCML* promoters using TBtools software [54].

4.5. RNA-seq of the CrCaMs/CrCMLs in Different C. rosea Tissues or under Different Stress Treatments

Tissue-specific expression profile analyses during different developmental stages of the *C. rosea* *CrCaMs*/*CrCMLs* was conducted using Illumina HiSeq X sequencing technology. Five different tissues from *C. rosea* plants (root, vine, young leaf, flower bud, and young silique samples) were collected from *C. rosea* adult plants and seedlings growing in the SCNBG. Mature leaf samples from *C. rosea* growing in SCNBG and on YX Island were examined using FastQC (http://www.bioinformatics.babraham.ac.uk/projects/fastqc/, accessed on 10 April 2024) based on the primary 40 Gb clean reads and were mapped to the *C. rosea* reference genome using Tophat v.2.0.10 (http://tophat.cbcb.umd.edu/, accessed on 10 April 2024). For the expression profiles of the *CrCaMs*/*CrCMLs* under different abiotic stressors, *C. rosea* seedling tissues (including leaves and roots) were also collected and sequenced at the transcriptome level. All of the expressed sequence tag (EST) information was then mapped to the *C. rosea* reference genome. Gene expression levels were calculated as fragments per kilobase (kb) of transcript per million mapped reads (FPKM) according to the length of the gene and the read counts mapped to the gene: FPKM = total exon fragments/[mapped reads (millions) × exon length (kb)]. The expression levels of the *CrCaMs*/*CrCMLs* were visualized as clustered heatmaps of log2 (FPKM + 1) values using TBtools. The FPKM values for all samples are listed in Table S3.

4.6. Expression Pattern Analysis Using Quantitative Reverse Transcription (qRT)-PCR

The total RNA was extracted from C. rosea tissues for the qRT-PCR assays using the EasyPure® Plant RNA Kit (TransGen Biotech, Beijing, China), and the cDNA was then synthesized using cDNA Synthesis SuperMix (TransGen Biotech, Beijing, China) according to the manufacturer's instructions. Quantitative RT-PCR was conducted using the LightCycler480 system (Roche, Basel, Switzerland) and TransStart Tip Green qPCR SuperMix (TransGen Biotech, Beijing, China). Reaction systems were prepared in 10-μL volumes as follows: 5 μL of 2 × Tip Green qPCR SYBR Master Mix, 0.5 μL of the forward primer (10 μM), 0.5 μL of the reverse primer (10 μM), 1 μL of cDNA (20 to 50 ng μL^{-1}), and 3 μL of RNase-free water. Each sample was tested using three technical replicates to ensure the accuracy of the results. There were three biological replicates per treatment. The primers used for the qRT-PCR were designed by Primer 3.0 and are listed in supplementary Table S1. The *CrEF-1α* gene was used as a reference, and the $2^{-\Delta\Delta CT}$ method was used to calculate the relative changes in gene expressions between the control and treatment plants [39].

4.7. Functional Identification Using a Yeast Expression System

The open reading frames (ORFs) of the *CrCaMs*/*CrCMLs* were PCR amplified from different cDNA samples of *C. rosea* with gene-specific primer pairs (listed in Table S1). After several PCR procedures, the PCR fragments were purified and cloned into the *Bam*HI and *Eco*RI sites of pYES2 to yield recombinant plasmids of CrCaMs/CrCMLs-pYES2 and sequenced. The *Saccharomyces cerevisiae* wild-type (WT) strain BY4741 (Y00000) and mutant strain *skn7Δ* (Y02900) were obtained from Euroscarf (http://www.euroscarf.de). The plasmids were introduced into yeast using the LiAc/PEG method. Yeast growth and stress tolerance tests were performed as previously described [16,33].

Single colonies of yeast transformants were selected and used to inoculate a liquid synthetic drop-out uracil medium with a 2% galactose (SDG-Ura) medium. It was then incubated overnight or longer at 30°C, diluted with fresh pre-warmed SDG medium (volume ratio 1:10), and incubated with vigorous shaking for approximately 30 h at 30°C to reach an optical density of one at OD600 (optical density at 600 nm). The cells were then serially diluted in 10-fold steps, and 2-μL of aliquots of each was finally spotted onto the SDG medium plates with or without stressors. To determine the heat tolerance, the liquid yeast cultures were incubated in a constant temperature bath (52°C) for different durations (*skn7Δ* for 15 and 20 min). The cultures were then spotted on solid SDG medium plates. The plates were incubated at 30°C for two to five days and photographed.

4.8. Statistical Analyses

All analyses were conducted at least in triplicate, and the results are shown as the means ± SDs (n ≥ 3). The Excel 2010 (Microsoft Corporation, Albuquerque, NM, USA) statistics program was used to perform the statistical analyses.

Supplementary Materials: The following supporting information can be downloaded at: www.mdpi.com/xxx/s1, Figure S1: The 3D models of 51 CrCaMs/CrCMLs constructed using Phyre2 (http://www.sbg.bio.ic.ac.uk/~phyre2/html/page.cgi?id=index); Table S1: Primer lists used in this study and the sequences information of *CrCaMs*/*CrCMLs*' genomic DNA, CDS, and promoter region DNA; Table S2: *Cis*-acting elements (CEs) analysis of *CrCaMs*' and *CrCMLs*' promoters; Table S3: FPKM values of *CrCaMs*/*CrCMLs* for RNA-Seq assay of *C. rosea* tissues in this study.

Author Contributions: Conceptualization, M.Z. and S.J.; methodology, M.Z.; software, Z.W.; validation, Q.D., Z.H. and M.Z.; formal analysis, Q.D., Z.W. and M.Z.; investigation, M.Z. and S.J.; resources, S.J.; data curation, M.Z.; writing—original draft preparation,Q.D., Z.H. and M.Z.; writing—review and editing, M.Z.; visualization, Q.D., Z.H. and M.Z.; supervision, S.J.; project administration, S.J.; funding acquisition, M.Z., Z.W. and S.J. All authors have read and agreed to the published version of the manuscript.

Funding: This research was funded by the National Natural Sciences Foundation of China (32270380), the Guangdong Science and Technology Program (2024B1212050007), the Key Special Project for Introduced Talents Team of Southern Marine Science and Engineering Guangdong Laboratory (Guangzhou) (GML2019ZD0408), and the funding from the Institution of South China Sea Ecology and Environmental Engineering, Chinese Academy of Sciences (ISEE2021ZD04). The funders had no roles in the study design, data collection and analysis, decision to publish, or preparation of the manuscript.

Conflicts of Interest: The authors declare no conflicts of interest.

References

1. Ranty, B.; Aldon, D.; Cotelle, V.; Galaud, J.P.; Thuleau, P.; Mazars, C. Calcium sensors as key hubs in plant responses to biotic and abiotic stresses. *Front. Plant Sci.* **2016**, 7, 327. [CrossRef]
2. McCormack, E.; Tsai, Y.C.; Braam, J. Handling calcium signaling: Arabidopsis CaMs and CMLs. *Trends Plant Sci*. **2005**, 10, 383–389. [CrossRef]
3. Zhu, X.; Dunand, C.; Snedden, W.; Galaud, J.P. CaM and CML emergence in the green lineage. *Trends Plant Sci*. **2015**, 20 (8), 483–489. [CrossRef]
4. Luan, S.; Kudla, J.; Rodriguez-Concepcion, M.; Yalovsky, S.; Gruissem, W. Calmodulins and calcineurin B-like proteins: calcium sensors for specific signal response coupling in plants. *Plant Cell* **2002**, 14, S389–400. [CrossRef]
5. White, P.J.; Broadley, M.R. Calcium in plants. *Ann. Bot*. **2003**, 92 (4), 487–511. [CrossRef]
6. Ketehouli, T.; Nguyen Quoc, V.H.; Dong, J.; Do, H.; Li, X.; Wang, F. Overview of the roles of calcium sensors in plants' response to osmotic stress signalling. *Funct. Plant Biol.* **2022**, 49 (7), 589–599. [CrossRef]
7. Chin, D.; Means, A.R. Calmodulin: a prototypical calcium sensor. *Trends Cell Biol*. **2000**, 10, 322–328. [CrossRef]
8. La-Verde, V.; Dominici, P.; Astegno, A. Towards understanding plant calcium signaling through calmodulin-like proteins: a biochemical and structural perspective. *Int. J. Mol. Sci*. **2018**, 19, 1331. [CrossRef]
9. Mohanta, T.K.; Kumar, P.; Bae, H. Genomics and evolutionary aspect of calcium signaling event in calmodulin and calmodulin-like proteins in plants. *BMC Plant Biol*. **2017**, 17, 38. [CrossRef]
10. Virdi, A.S.; Singh, S.; Singh, P. Abiotic stress responses in plants: roles of calmodulin-regulated proteins. *Front. Plant Sci*. **2015**, 6, 809. [CrossRef]
11. He, M.; He, H.C.Q.; Ding, N.Z. Abiotic stresses: general defenses of land plants and chances for engineering multistress tolerance. *Front. Plant Sci*. **2018**, 9, 1771. [CrossRef]

12. McCormack, E.; Braam, J. Calmodulins and related potential calcium sensors of Arabidopsis. *New Phytol*. **2003**, 159 (3), 585–598. [CrossRef]
13. Boonburapong, B.; Buaboocha, T. Genome-wide identification and analyses of the rice calmodulin and related potential calcium sensor proteins. *BMC Plant Biol*. **2007**, 7, 4. [CrossRef]
14. Li, Q.; Gao, L.; Yu, F.; Lü, S.; Yang P. Evolution and diversification of *CaM/CML* gene family in green plants. *Plant Physiol*. *Biochem*. **2023**, 202, 107922. [CrossRef]
15. Huang, J.; Liu, N.; Ren, H.; Jian, S.G. Physiology and biochemical characteristics of *Canavalia maritim*e under stress. *J. Trop*. *Subtrop*. *Bot*. **2019**, 27 (02), 157–163. [CrossRef]
16. Lin, R.; Zheng, J.; Pu, L.; Wang, Z.; Mei, Q.; Zhang, M.; Jian, S. Genome-wide identification and expression analysis of *aquaporin* family in *Canavalia rosea* and their roles in the adaptation to saline-alkaline soils and drought stress. *BMC Plant Biol*. **2021**, 21 (1), 333. [CrossRef]
17. Jia, .L; Chu, H.; Wu, D.; Feng, M.; Zhao, L. Role of calmodulin in thermotolerance. *Plant Signal Behav*. **2014**, 9, e28887. [CrossRef]
18. Zeng, H.; Xu, L.; Singh, A.; Wang, H.; Du, L.; Poovaiah, B.W. Involvement of calmodulin and calmodulin-like proteins in plant responses to abiotic stresses. *Front*. *Plant Sci*. **2015**, 6, 600. [CrossRef]
19. Ranty, B.; Aldon, D.; Cotelle, V.; Galaud, J.P.; Thuleau, P.; Mazars, C. Calcium sensors as key hubs in plant responses to biotic and abiotic stresses. *Front*. *Plant Sci*. **2016**, 7, 327. [CrossRef]
20. Wang, L.; Liu, Z.; Han, S.; Liu, P.; Sadeghnezhad, E.; Liu, M. Growth or survival: what is the role of calmodulin-like proteins in plant? *Int*. *J*. *Biol*. *Macromol*. **2023**, 242 (Pt1), 124733. [CrossRef]
21. Shen, Q.; Fu, L.; Su, T.; Ye, L.; Huang, L.; Kuang, L.; Wu, L.; Wu, D.; Chen, Z.H.; Zhang G. Calmodulin HvCaM1 negatively regulates salt tolerance via modulation of HvHKT1s and HvCAMTA4. *Plant Physiol*. **2020**, 183 (4), 1650–1662. [CrossRef]
22. Yang, S.; Xiong, X.; Arif, S.; Gao, L.; Zhao, L.; Shah, I.H.; Zhang, Y. A calmodulin-like *CmCML13* from *Cucumis melo* improved transgenic *Arabidopsis* salt tolerance through reduced shoot's Na$^+$, and also improved drought resistance. *Plant Physiol*. *Biochem*. **2020**, 155, 271–283. [CrossRef]
23. Du, B.; Chen, N.; Song, L.; Wang, D.; Cai, H.; Yao, L.; Li, X.; Guo, C. Alfalfa (*Medicago sativa* L.) *MsCML46* gene encoding calmodulin-like protein confers tolerance to abiotic stress in tobacco. *Plant Cell Rep*. **2021**, 40 (10), 1907–1922. [CrossRef]
24. Jamra, G.; Agarwal, A.; Singh, N.; Sanyal, S.K.; Kumar, A.; Pandey, G.K. Ectopic expression of finger millet calmodulin confers drought and salinity tolerance in *Arabidopsis thaliana*. *Plant Cell Rep*. **2021**, 40 (11), 2205–2223. [CrossRef]
25. Zhang, Y.; Huang, J.; Hou, Q.; Liu, Y.; Wang, J.; Deng, S. Isolation and functional characterization of a salt-responsive calmodulin-like gene *MpCML40* from semi-mangrove *Millettia pinnata*. *Int*. *J*. *Mol*. *Sci*. **2021**, 22 (7), 3475. [CrossRef]
26. Hau, B.; Symonds, K.; Teresinski, H.; Janssen, A.; Duff, L.; Smith, M.; Benidickson, K.; Plaxton, W.; Snedden, W.A. Arabidopsis calmodulin-like proteins CML13 and CML14 interact with calmodulin-binding transcriptional activators and function in salinity stress response. *Plant Cell Physiol*. **2024**, 65 (2), 282–300. [CrossRef]
27. Raina, M.; Kumar, A.; Yadav, N.; Kumari, S.; Yusuf, M.A.; Mustafiz, A.; Kumar, D. StCaM2, a calcium binding protein, alleviates negative effects of salinity and drought stress in tobacco. *Plant Mol*. *Biol*. **2021**, 106 (1–2), 85–108. [CrossRef]
28. Yang, M.; Zhou, B.; Song, Z.; Tan, Z.; Liu, R.; Luo, Y.; Guo, Z.; Lu, S. A calmodulin-like protein PvCML9 negatively regulates salt tolerance. *Plant Physiol*. *Biochem*. **2024**, 210, 108642. [CrossRef]
29. Xue, N.; Sun, M.; Gai, Z.; Bai, M.; Sun, J.; Sai, S.; Zhang, L. Genome-wide identification and expression analysis of *calmodulin* (*CaM*) and *calmodulin-like* (*CML*) genes in the brown algae *Saccharina japonica*. *Plants (Basel)* **2023**, 12 (10), 1934. [CrossRef]
30. Gao, L.; Damaris, R.N.; Yu, F.; Yang, P.F. Genome-wide identification and expression analysis of *CaM/CML* gene family in sacred lotus (*Nelumbo nucifera*). *Plant Mol*. *Biol*. *Rep*. **2022**, 40, 418–432. [CrossRef]
31. Yang, M.; Chen, J.; Liu, T.; Xiang, L.; Zhou, B.F. Genome-wide identification and expression analysis of calmodulin-like gene family in *Paspalums vaginatium* revealed their role in response to salt and cold stress. *Curr*. *Issues Mol*. *Biol*. **2023**, 45 (2), 1693–1711. [CrossRef]
32. Wu, X.; Zhu, J.; Zhu, L.; Tang, Y.; Hao, Z.; Zhang, J.; Shi, J.; Cheng, T.; Lu, L. Genome-wide analyses of calmodulin and calmodulin-like proteins in the halophyte *Nitraria sibirica* reveal their involvement in response to salinity, drought and cold stress. *Int*. *J*. *Biol*. *Macromol*. **2023**, 253 (Pt7), 127442. [CrossRef]
33. Lin, R.; Zou, T.; Mei, Q.; Wang, Z.; Zhang, M.; Jian, S. Genome-wide analysis of the *late embryogenesis abundant* (*LEA*) and *abscisic acid-, stress-, and ripening-induced* (*ASR*) gene superfamily from *Canavalia rosea* and their roles in salinity/alkaline and drought tolerance. *Int*. *J*. *Mol*. *Sci*. **2021**, 22 (9), 4554. [CrossRef]
34. Zhang, M.; Jian, S.; Wang, Z. Comprehensive analysis of the *Hsp20* gene family in *Canavalia rosea* indicates its roles in the response to multiple abiotic stresses and adaptation to tropical coral islands. *Int*. *J*. *Mol*. *Sci*. **2022**, 23 (12), 6405. [CrossRef]

35. Zhang, M.; Wang, Z.; Jian, S. Functional characterization of *heat shock factor* (*CrHsf*) families provide comprehensive insight into the adaptive mechanisms of *Canavalia rosea* (Sw.) DC. to tropical coral islands. *Int. J. Mol. Sci.* **2022**, 23 (20), 12357. [CrossRef]
36. Zou, T.; Lin, R.; Pu, L.; Mei, Q.; Wang, Z.; Jian, S.; Zhang, M. Genome-wide identification, structure characterization, expression pattern profiling, and substrate specificity of the metal tolerance protein family in *Canavalia rosea* (Sw.) DC. *Plants (Basel)* **2021**, 10 (7), 1340. [CrossRef]
37. Zou, T.; Pu, L.; Lin, R.; Mo, H.; Wang, Z.; Jian, S.; Zhang, M. Roles of *Canavalia rosea* metallothioneins in metal tolerance and extreme environmental adaptation to tropical coral reefs. *J. Plant Physiol.* **2022**, 268, 153559. [CrossRef]
38. Zhang, M.; Wang, Z.; Jian, S. Genome-wide identification and functional analysis of the *GASA* gene family responding to multiple stressors in *Canavalia rosea*. *Genes (Basel)* **2022**, 13 (11), 1988. [CrossRef]
39. Ding, Q.; Liu, H.; Lin, R.; Wang, Z.; Jian, S.; Zhang, M. Genome-wide functional characterization of *Canavalia rosea cysteine-rich trans-membrane module* (*CrCYSTM*) genes to reveal their potential protective roles under extreme abiotic stress. *Plant Physiol. Biochem.* **2023**, 200, 107786. [CrossRef]
40. Goldtzvik, Y.; Sen, N.; Lam, S.D.; Orengo, C. Protein diversification through post-translational modifications, alternative splicing, and gene duplication. *Curr. Opin. Struct. Biol.* **2023**, 81, 102640. [CrossRef]
41. Das Laha, S.; Dutta, S.; Schäffner, A.R.; Das, M. Gene duplication and stress genomics in Brassicas: Current understanding and future prospects. *J. Plant Physiol.* **2020**, 255, 153293. [CrossRef]
42. Martins, T.S.; Da-Silva, C.J.; Shabala, S.; Striker, G.G.; Carvalho, I.R.; de Oliveira, A.C.B.; do Amarante, L. Understanding plant responses to saline waterlogging: insights from halophytes and implications for crop tolerance. *Planta* **2023**, 259 (1), 24. [CrossRef]
43. Li, C.Y.; He, R.; Tian, C.Y.; Song, J. Utilization of halophytes in saline agriculture and restoration of contaminated salinized soils from genes to ecosystem: *Suaeda salsa* as an example. *Mar. Pollut. Bull.* **2023**, 197, 115728. [CrossRef]
44. Liang, X.; Li, J.; Yang, Y.; Jiang, C.; Guo, Y. Designing salt stress-resilient crops: Current progress and future challenges. *J. Integr. Plant Biol.* **2024**, 66 (3), 303–329. [CrossRef]
45. McAinsh, M.R.; Pittman, J.K. Shaping the calcium signature. *New Phytol.* **2009**, 181 (2), 275–294. [CrossRef]
46. Sanders, D.; Brownlee, C.; Harper, J.F. Communicating with calcium. *Plant Cell* **1999**, 11 (4), 691–706. [CrossRef]
47. Liao, J.; Deng, J.; Qin, Z.; Tang, J.; Shu, M.; Ding, C.; Liu, J.; Hu, C.; Yuan, M.; Huang, Y.; Yang, R.; Zhou, Y. Genome-wide identification and analyses of calmodulins and calmodulin-like proteins in *Lotus japonicus*. *Front. Plant Sci.* **2017**, 8, 482. [CrossRef]
48. Sun, Q.; Yu, S.; Guo, Z. Calmodulin-Like (CML) Gene family in *Medicago truncatula*: genome-wide identification, characterization and expression analysis. *Int. J. Mol. Sci.* **2020**, 21 (19), 7142. [CrossRef]
49. Yadav, M.; Pandey, J.; Chakraborty, A.; Hassan, M.I.; Kundu, J.K.; Roy, A.; Singh, I.K.; Singh, A. A comprehensive analysis of calmodulin-Like proteins of *Glycine max* indicates their role in calcium signaling and plant defense against insect attack. *Front. Plant Sci.* **2022**, 13, 817950. [CrossRef]
50. Zhao, H.; Gao, Y.; Du, Y.; Du, J.; Han, Y. Genome-wide analysis of the *CML* gene family and its response to melatonin in common bean (*Phaseolus vulgaris* L.). *Sci. Rep.* **2023**, 13 (1), 1196. [CrossRef]
51. Sun, Q.; Huang, R.; Zhu, H.; Sun, Y.; Guo, Z. A novel Medicago truncatula calmodulin-like protein (MtCML42) regulates cold tolerance and flowering time. *Plant J.* **2021**, 108 (4), 1069–1082. [CrossRef]
52. Fu, N.; Wang, L.; Han, X.; Yang, Q.; Zhang, Y.; Tong, Z.; Zhang, J. Genome-wide identification and expression analysis of calmodulin and calmodulin-like genes, revealing *CaM3* and *CML13* participating in drought stress in *Phoebe bournei*. *Int. J. Mol. Sci.* **2023**, 25 (1), 545. [CrossRef]
53. Nei, M.; Gojobori, T. Simple methods for estimating the numbers of synonymous and nonsynonymous nucleotide substitutions. *Mol. Biol. Evol.* **1986**, 3 (5), 418–426. [CrossRef]
54. Chen, C.; Chen, H.; Zhang, Y.; Thomas, H.R.; Frank, M.H.; He, Y.; Xia, R. TBtools: an integrative toolkit developed for interactive analyses of big biological data. *Mol. Plant.* **2020**, 13 (8), 1194–1202. [CrossRef]